

**Simulation Study on Utilisation of Biogas from Palm Oil Mill Effluent  
(POME) as Fuel for Diesel Generator Set**

by

Meveeqhen A/L Ravi Chandran

22823

Dissertation submitted in partial fulfilment  
of the requirements for the  
Bachelor of Mechanical Engineering  
With Honours

FYP II  
January 2020

Universiti Teknologi PETRONAS  
32610 Seri Iskandar  
Perak Darul Ridzuan

CERTIFICATION OF APPROVAL

**Simulation Study on Utilisation of Biogas from Palm Oil Mill Effluent  
(POME) as Fuel for Diesel Generator Set**

by

Meveeqhen A/L Ravi Chandran

22823

A project dissertation submitted to the  
Mechanical Engineering Programme  
Universiti Teknologi PETRONAS  
in partial fulfilment of the requirement for the  
BACHELOR OF ENGINEERING (Hons)  
(MECHANICAL)

Approved by,



---

(AP Ir. Dr. Suhaimi Hassan)

UNIVERSITI TEKNOLOGI PETRONAS  
TRONOH, PERAK  
January 2020

## CERTIFICATION OF ORIGINALITY

This is to certify that I am responsible for the work submitted in this project, that the original work is my own except as specified in the references and acknowledgements, and that the original work contained herein have not been undertaken or done by unspecified sources or persons.



---

MEVEEQHEN A/L RAVI CHANDRAN

## ABSTRACT

Biogas harnessed from the liquid by-product of palm oil production is widely used for power generation. Dual-fuel engines incorporate biogas as primary fuel and diesel as pilot fuel to facilitate advanced combustion strategies. This study presents a simulation study of biogas utilisation in dual fuel mode conducted on a diesel generator set in IOI Pukin Palm Oil Mill, Rompin, Pahang. In this paper, the maximum substitution level of diesel with biogas for the proposed dual-fuel engine is presented. The CFD combustion simulation was performed using ANSYS Forte IC Engine software to study the effect of biogas substitution on in-cylinder peak pressure, maximum temperature, chemical rate of heat release (RoHR) and emission characteristics for six different biogas-diesel compositions. For turbulence analysis, RNG  $\kappa$ - $\epsilon$  model was employed whereas default models were used to study other combustion parameters. The optimum engine load for dual-fuel operation was found to be 75% with 486kW power output based on theoretical calculations of brake thermal efficiency, specific fuel consumption and diesel replacement ratio. The CFD combustion simulation results show that values of all combustion parameters decreased with higher biogas substitution (by volume). However, a significantly large drop in RoHR was found between the 80/20 and 85/15 biogas-diesel mix. Therefore, since RoHR is directly proportional to BTE, the 80/20 mix was selected as the optimum composition for the proposed dual-fuel engine. Emission analysis for the 80/20 mix demonstrated a substantial 42% NO<sub>x</sub> reduction compared to pure diesel. The simulation results are in conformance with experimental results obtained from previous research studies. Hence, combustion and exhaust emission characteristics for the proposed dual-fuel engine was effectively determined through the CFD simulation study in this paper. Future work to investigate engine stability and knocking of the proposed dual fuel engine using 80% biogas-20% diesel is recommended.

## **ACKNOWLEDGEMENT**

At the beginning of this report, allow me to seize this opportunity to recognize and express my wholehearted gratitude towards a few parties that enabled me to successfully complete this final dissertation.

My deepest appreciation first goes to Associate Professor Ir. Dr. Suhaimi Hassan who expertly guided me throughout both final year project (FYP) semesters. His unwavering enthusiasm in this field of study kept me constantly engaged with my research which progressed to the formulation of methodology and eventually the interpretation, analysis and discussion of the results obtained.

Next, I would like to thank the management of IOI Pukin Palm Oil Mill mainly the mill manager, Mr. Kesavan Manohar and assistant mill manager, Mr Kunalan Nadaraj for providing the required industrial data and necessary guidance to successfully execute this project.

Last but not least, I would like to sincerely show my appreciation to the Mechanical Engineering Department of Universiti Teknologi PETRONAS (UTP), mainly toward course coordinators Dr. Tamiru and Dr. Akililu for administering the final year project across two semesters.

## TABLE OF CONTENTS

<b>CERTIFICATION</b>	. . . . .	i
<b>ABSTRACT</b>	. . . . .	iii
<b>ACKNOWLEDGEMENT</b>	. . . . .	iv
<b>CHAPTER 1:</b>	<b>INTRODUCTION</b>	1
	1.1 Background of Study	1
	1.2 Problem Statement	4
	1.3.1 Objectives	4
	1.3.2 Scope of Study	5
<b>CHAPTER 2:</b>	<b>LITERATURE REVIEW</b>	6
	2.1 Overview of Palm Oil Industry in Malaysia	6
	2.2 General Palm Oil Mill Process	6
	2.3 Generation of Biogas	7
	2.4 Classification of Internal Combustion Engines	9
	2.5 Dual Fuel Engine Process and Applications	10
	2.6 CFD Simulation	12
	Summary	13
<b>CHAPTER 3:</b>	<b>METHODOLOGY</b>	14
	3.1 Research Methodology	14
	3.2 Engine Specifications	17
	3.3 Engine Performance Analysis.	17
	3.4 Steps Required for In-Cylinder Engine Simulation	18
	3.5 Project Planning	22
	Summary	27
<b>CHAPTER 4:</b>	<b>RESULTS AND DISCUSSION</b>	28
	4.1 Overview	28
	4.2 Mesh Independence Test	28
	4.3 Basis of Calculation	29
	4.4 Engine Performance Analysis.	32
	4.5 Effect of Engine Load and Biogas-Diesel Composition Variations on Dual Fuel CI engine	37
	4.6 CFD Simulation Results of Heat Transfer Analysis and In-Cylinder Combustion and Exhaust Emission Characteristics in Dual Fuel CI Engine	40
	4.7 Economic Analysis	50
<b>CHAPTER 5:</b>	<b>CONCLUSION AND RECOMMENDATION</b>	52
	5.1 Conclusion	52
	5.2 Recommendations	53
<b>REFERENCES</b>	. . . . .	54

## LIST OF FIGURES

Figure 1.1	Malaysian Renewable Energy Sources	2
Figure 2.1	Overall Process Flow in Pukin Palm Oil Mill	7
Figure 2.2	Stages of Anaerobic Digestion	8
Figure 2.3	Cross section of Dual Fuel CI Engine	11
Figure 2.4	Dual Fuel CI Engine Setup	11
Figure 3.1	Project Flow	16
Figure 3.2	Sector Mesh geometry from Enight	19
Figure 3.3	60-degree KIVA-sector mesh	20
Figure 3.4	Combustion Chamber 2D-view at TDC	20
Figure 3.5	Gantt Chart FYP I	23
Figure 3.6	Gantt Chart FYP II	25
Figure 4.1	Mesh Independent Solution Graph	29
Figure 4.2, 4.3, 4.4	Theoretical and Actual BTE ( $\eta = 20\%$ );( $\eta = 17\%$ );( $\eta = 23\%$ )	34- 36
Figure 4.5	Brake thermal efficiency against engine loads	37
Figure 4.6	Specific fuel consumption against engine loads	38
Figure 4.7	Diesel displacement ratio against engine loads	39
Figure 4.8 (a),(b),(c),(d), (e),(f)	Contours of In-Cylinder Peak Pressure	40- 41
Figure 4.9	Pressure vs Crank Angle Diagram	41
Figure 4.10 (a),(b),(c),(d), (e),(f)	Contours of In-Cylinder Maximum Temperature	42- 43
Figure 4.11	Maximum Temperature vs Crank Angle Diagram	43
Figure 4.12 (a),(b),(c),(d), (e),(f)	Contours of In-Cylinder Chemical RoHR	44- 45
Figure 4.13	RoHR vs Crank Angle at 80% biogas substitution	45
Figure 4.14	RoHR vs Crank Angle for various Biogas-Diesel Compositions	46
Figure 4.15	RoHR vs various Biogas-Diesel Compositions	47
Figure 4.16 (a),(b)	Contours of Exhaust NO <sub>x</sub> Emissions	48
Figure 4.17 (a),(b)	Contours of Exhaust CO Emissions	49

## LIST OF TABLES

Table 1.1	Fuel Mix for Electricity Generation in Malaysia	1
Table 3.1	Gen-Set Specifications	17
Table 3.2	General Procedure for Simulation Analysis	22
Table 3.3	Milestones (FYP I)	24
Table 3.4	Milestones (FYP II)	26
Table 4.1	Mesh Independence Test Results	28
Table 4.2	Data for Key Parameters used in Engine Calculations	29
Table 4.3	Theoretical Diesel Consumption for 648kW Gen Set (PPOM)	30
Table 4.4	Actual Diesel Consumption for 648kW Gen Set (PPOM)	31
Table 4.5	Theoretical and Actual BTE ( $\eta = 20\%$ )	33
Table 4.6	Theoretical and Actual BTE ( $\eta = 17\%$ )	34
Table 4.7	Theoretical and Actual BTE ( $\eta = 23\%$ )	35
Table 4.8	Yearly Diesel Fuel Consumption (648kW Gen-Set)	50



## ABBREVIATIONS AND NOMENCLATURE

$H_{biogas}$  – biogas heating value,  $\text{kJ kg}^{-1}$

$H_{diesel}$  – diesel heating value,  $\text{kJ kg}^{-1}$

$\dot{m}_{biogas}$  – mass flow rate of biogas,  $\text{kg s}^{-1}$

$\dot{m}_{diesel}$  - mass flow rate of diesel in normal diesel operation,  $\text{kg s}^{-1}$

$\dot{m}_{dual}$  - mass flow rate of diesel in dual-fuel operation,  $\text{kg s}^{-1}$

DRR – Diesel Replacement Ratio

$W$  – output power, kW

$\eta$  - thermal efficiency, %

BTE- brake thermal efficiency

CI - compression ignition

TDC - top dead center

ATDC - after top dead center

RoHR – rate of heat release

CH<sub>4</sub> – methane

CO<sub>2</sub> – carbon dioxide

H<sub>2</sub>S – hydrogen sulfide

PPOM - Pukin Palm Oil Mill

IVC – intake valve close

EVO – exhaust valve open

# CHAPTER 1 : INTRODUCTION

## 1.1 Background Study

In general, energy sources can be classified as renewable and non-renewable. Malaysia possesses both types of energy sources which is parallel to the nation's energy mix comprising of five-fuel diversification. Renewable energy sources are currently the most rapidly growing green energy alternatives for power generation. Despite many available resources, the country is still heavily reliant on fossil fuels usage across transportation and industrial sectors. Table 1.1 shows the sources of fuel used for electricity generation in Malaysia based on their percentages.

TABLE 1.1: Fuel Mix for Electricity Generation in Malaysia, 2015 [1]

Non- Renewable Energy	Coal	47%
	Natural Gas	23%
	Oil/Petroleum Products	2%
Renewable Energy	Hydropower	24%
	Solar	2.8%
	Biomass	0.96%
	Biogas	0.24%

Based on Table 1.1, fossil fuels such as coal, oil and natural gas still dominate the overall energy industry which poses an alarming depletion risk in the future hence renewable energy development is critical towards the environmental sustainability and energy security of Malaysia. The national energy demand is forecasted to have an annual rise of 4.7% whereby the usage of electricity will grow annually by 8.1% [2]. The Malaysian government has encouraged the enhancement of renewable energy technology by the implementation of multiple policies to escalate the national energy mix so that the country's dependence on fossil fuels can be lowered and also to encourage sustainable development.

The Eleventh Malaysia Plan (11MP) is a significant government initiative which supports the utilisation of renewable to heighten the energy security of the nation [3]. The 11MP has focused on promoting new renewable energy sources, enhancing its total installed capacity and also introduced net energy metering to strengthen green energy development. The 11MP emphasises on a better management of resources to ensure supply diversity hence the electricity subsectors can be well secured. This management strategy is aimed to gradually reduce the country's dependency on fossil fuels by fuel mix optimisation and alternative fuels exploration. Besides, the plan pursues renewable energy options with large potential such as biogas, mini hydro plants, solar PV and biomass to enhance alternative energy sources. Figure 1.1 illustrates the renewable energy sources in Malaysia.

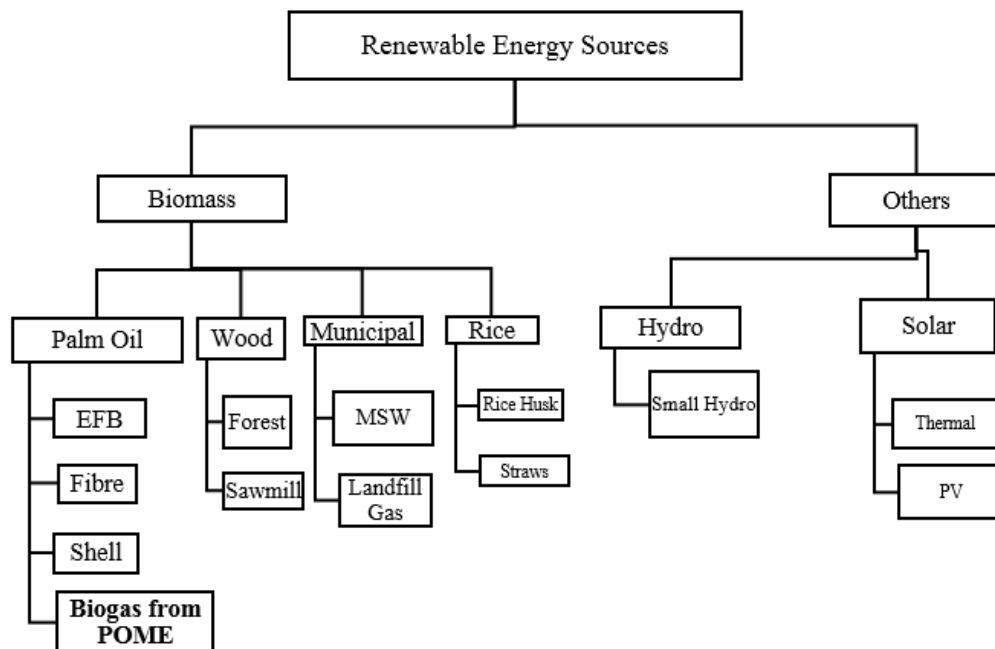


FIGURE 1.1: Malaysian Renewable Energy Sources [4]

To encourage the take-off of renewable energy, 11MP has effectively introduced net energy metering (NEM) which was launched by the Ministry of Energy, Science, Technology, Environment and Climate Change (KeTTHA). NEM prioritises internal consumption in production sites prior to feeding any excess power generated to the grid therefore encouraging industrial plants such as mills to produce power free from any restriction on the production capacity. Under the National Renewable Energy Policy and Action Plan (NREPAP) [5], which was introduced in 2009, it is expected

by the year 2020, electricity produced from green energy will reach 11,227GWh. In Peninsular Malaysia, the total installed capacity of renewable energy power stations was 2,244.38 MW and 4,181.89 GWh of electricity was generated in 2017, of which 81.57% were from natural gas, 16.39% were from renewable energy and the remainder was petroleum products. Among these resources, biogas which is derived from biomass, is of great interest as it has a high potential to strengthen our nation's energy security by its utilisation to generate electricity [7] and simultaneously combat waste accumulation.

Currently, biogas is making big strides in local engineering industries as a source of gaseous fuel where it is harnessed using trapping facilities. Malaysia is determined to lower its carbon dioxide emissions by 40% in 2020 [3] hence biogas holds a strong potential of biogas to displace diesel in reducing the highly polluting black smoke and particulate emissions given out by high diesel usage which worsens the industrial carbon footprint. Biogas is released from wastewater treatment plants and is feasible for continuous combustion in engine cylinders.

Biogas is a source of primary renewable energy and if effluent treatment plants are not properly managed to trap methane, it will pose issues to the carbon footprint because methane is 25 times more potent compared to carbon dioxide as a dangerous greenhouse gas. A method commonly used throughout palm oil mills is open flaring where the biogas is wastefully flared into the atmosphere. However, with a biogas recovery plant to effectively trap methane, the harnessed biogas can be strongly utilised as a gaseous fuel to generate electricity.

Moreover, biogas holds a significant advantage due to its unending generation from palm oil processing. Hence, biogas is always available for usage as it is readily harnessed from liquid waste in palm oil production known as palm oil mill effluent (POME). As compared to using natural gas for energy, using biogas is more cost effective as natural gas involves extraction costs, while biogas is ready to be used as fuel. It will inevitably be a stable investment to invest in biogas as a gaseous fuel for power generation as the emission of methane from effluent treatment plants are highly predictable over years, and does not pose a risk of complete depletion such as wind and other types of renewable energies. Biogas, when used in compressed form can substitute compressed natural gas (CNG) and liquefied petroleum gas (LPG). Biogas

utilisation in power generation provides many benefits. Biogas is a clean fuel which restrains engine oil contaminants and generates lower amount of harmful exhaust emissions to the atmosphere through cleaner combustion.

## **1.2 Problem Statement**

Biogas generation from the recovery plant of Pukin Palm Oil Mill started from the year 2017. Until today, only 80% biogas is fed and combusted in the boiler whereas the remaining 20% is openly flared. The excess biogas can be alternatively utilised for power generation instead of wastefully open flaring to the atmosphere. Considering the mill operates its diesel generator set on pure diesel, the smoke and particulate emissions that are exhausted to the atmosphere contribute to a higher carbon footprint. Therefore, it is proposed to conduct a study to estimate the utilization of biogas in dual fuel operation for the diesel generator set as a potential solution to prevent waste of biogas from open flaring.

### **1.3.1 Objectives**

- 1) To study the generation of biogas in Pukin Palm Oil Mill (PPOM)
- 2) To simulate the utilization of biogas in a dual-fuel mode on the existing diesel generator set in Pukin Palm Oil Mill (PPOM)
- 3) To conduct CFD combustion simulation of a diesel engine in dual fuel mode for analysis of in-cylinder combustion and exhaust emission characteristics

### **1.3.2 Scope of Study**

As the palm oil industry has a vast scope comprising of plantations, mills and refineries, this project emphasises on the utilisation of biogas from palm oil mill effluent (POME) into a 648kW diesel generator set located in the power generation station (engine room) of PPOM. The diesel generator set is proposed to run on a dual fuel mode with biogas as primary fuel and diesel as pilot fuel. This research will specifically cover the simulation analysis of combustion and exhaust emission characteristics between diesel and biogas-air mixture in a 60-degree sector geometry (1/6 of the cylinder). In the heat transfer analysis, key combustion parameters such as maximum temperature, peak pressure, chemical rate of heat release (RoHR) as well as NO<sub>x</sub> and CO emissions rates are studied. Furthermore, this project aims to develop a framework in which the maximum substitution level of diesel with biogas for the proposed dual fuel engine can be effectively determined.

## **CHAPTER 2 : LITERATURE REVIEW**

### **2.1 Overview of Palm Oil Mill Industry in Malaysia**

The Malaysian palm oil industry has been vastly developed and stands tall as one of the world's biggest producers and exporters, owning 454 palm oil mills distributed across a landbank of approximately 5.81 million hectares. Malaysia generated 39% of world palm oil production and 44% of exports globally in the year 2017 [5]. However, the aftermath of palm oil processing include solid and liquid by-products such as palm kernel shell (PKS), empty fruit bunches (EFB), mesocarp fiber and palm oil mill effluent (POME). Figuratively, a hectare of raw material known as fresh fruit bunches (FFB) can yield 50–70 tons of biomass residues after they undergo production [6]. In Malaysia, the Big Four Planters, namely Felda Global Ventures, Sime Darby, IOI Corporation Berhad and Genting Berhad, generate one third of the total crude palm oil.

The focus of this case study is on IOI Corporation Berhad, with 15 palm oil mills nationwide processing roughly 4.6 million tonnes of fresh fruit bunches (FFB) yearly with a land bank of 156,957 hectares. IOI Pukin Palm Oil Mill (PPOM), is one of the four mills located in Peninsular Malaysia. Pukin Palm Oil Mill is situated at 30km Lebu Raya Tun Razak, Keratong, Rompin, Pahang. The total plant size of the mill is 19.16 hectares with a throughput capacity of 60 mt/hr of FFB processed. Crude palm oil and palm kernels are the main products produced by PPOM. In terms of workforce, 105 employees contribute to the mill operations, with a breakdown of 28 staffs and 77 workers.

### **2.2 General Palm Oil Mill Process**

Pukin Palm Oil Mill has 13 stations all together. The stations include FFB (raw material) loading bay, sterilization (CMC), threshing, pressing, clarification, nut and kernel plant, water treatment plant, laboratory, effluent treatment plant, boiler, engine room (power house), biogas recovery plant, and the mechanical and electrical workshop as illustrated in Figure 2.1.

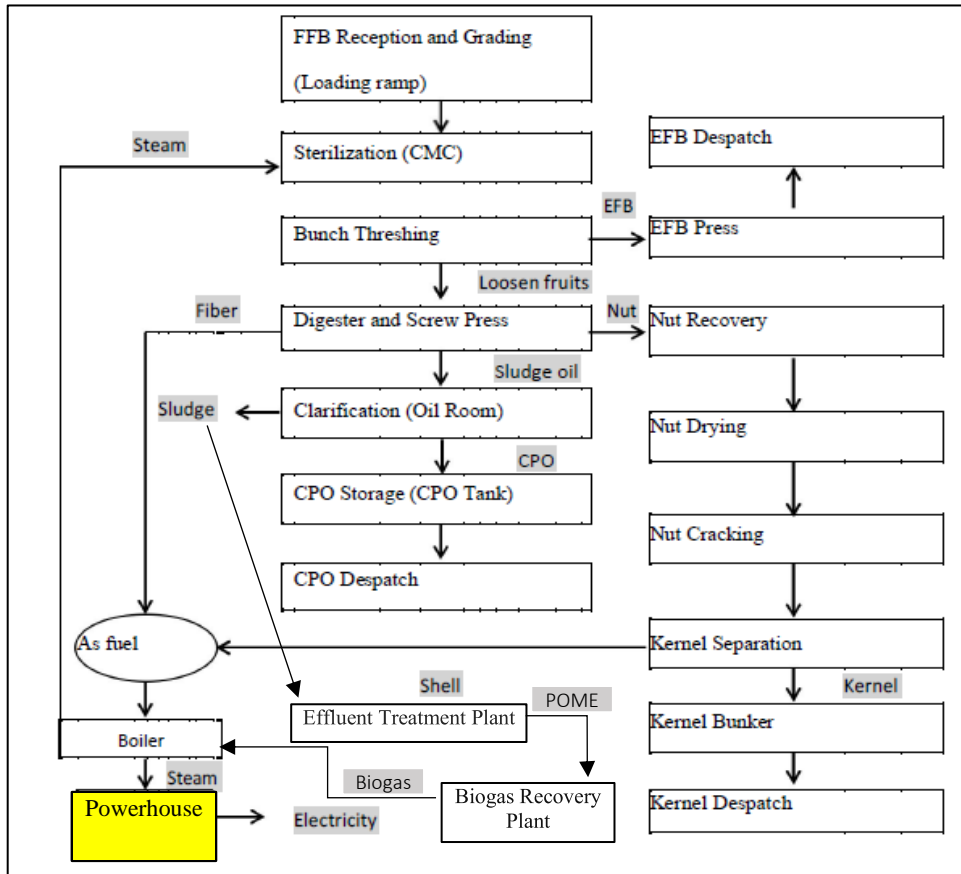


FIGURE 2.1: Overall Process Flow in Pukin Palm Oil Mill [6]

Based on the illustration in Figure 2.1, the areas of interest in this project is mainly the powerhouse, which is also known as the engine room as well as the biogas recovery plant. The powerhouse features a 2000kW turbine and three diesel generators for electricity generation (400kW, 400kW and 648kW). The biogas recovery plant harnesses methane from the wastewater effluent and channels it for burning to the water tube boiler.

### 2.3 Generation of Biogas

Biogas is the main product of anaerobic digestion in a covered lagoon of the liquid waste known as palm oil mill effluent (POME) [7]. During anaerobic digestion, the bacteria of organic matter in POME undergoes decomposition into biogas. This treatment occurs in anoxic conditions where oxygen concentrations are depleted. In this anaerobic environment, there is a large extraction of biological oxygen demand (BOD) as a combination of mainly carbon dioxide and methane in gaseous form. Therefore, corrosive hydrogen sulphide gas in the lagoon is released due to formation of septic conditions. Acid-forming bacteria causes most of of such degradation. The



process of anaerobically digesting organic molecules happen in following four main stages shown in Figure 2.2.

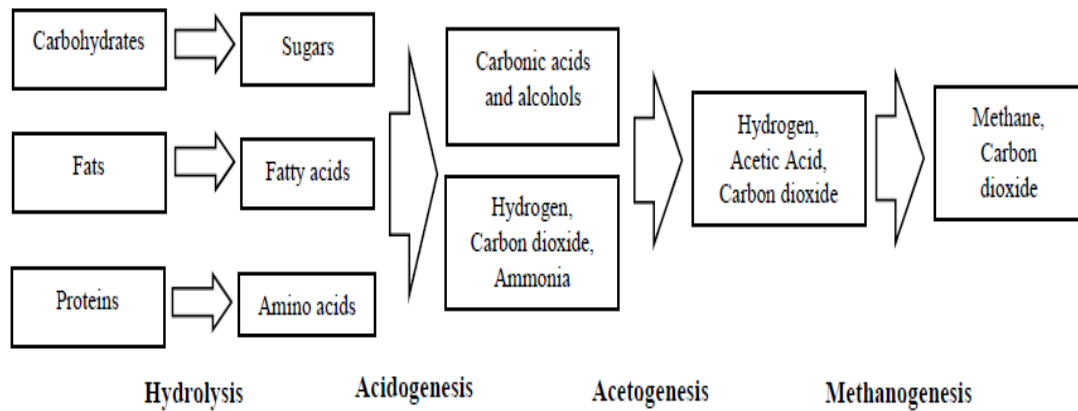


FIGURE 2.2 : Stages of Anaerobic Digestion [6]

Biogas composition in POME is constituted of 55-65% methane, 28-34% carbon dioxide and very minor hydrogen sulfide concentrations [8]. The CH<sub>4</sub> content in biogas from POME dominates different biogas sources such as landfill, animal manure and sewage sludge. [9] In global warming, methane gas emissions are 25 times more powerful than CO<sub>2</sub>, which increases the carbon footprint. Biogas density is about 1.2 kg/m<sup>3</sup>, which approximately equals that of air at ambient condition. Due to that, it needs a higher storage volume instead of being compressed. Biogas critical pressure ranges from 75-98 bar and its critical temperature is 82.5°C. This proves that when biogas is compressed to a critical state, it can transform from gaseous to liquid phase.

Biogas becomes a homogeneous fuel with a heat capacity surpassing 24 MJ/m<sup>3</sup> after carbon dioxide is removed. In terms of calorific value, methane is the most pivotal component in biogas. The estimated electricity potential from biogas in the year 2015 was 100MW [10] and possess 360–400 MW of energy reserve in the year 2020 with 410MW forecasted by the year 2030 [2].

Biogas trapping facilities are amongst the palm oil industry's eight Entry Point Projects (EPPs) that were first executed under the Palm Oil National Key Economic Area (NKEA) [7] in the Economic Transformation Programme (ETP) in the year 2010 with the Malaysian Palm Oil Board (MPOB) as the implementing

agency. It is estimated that over 17–20 million tonnes of CO<sub>2</sub> equivalent of GHG can be mitigated each year if continuous biogas trapping was practised by all mills [4]. Furthermore, biogas can be utilised for multiple energy applications.

## **2.4 Classification of Internal Combustion Engines (ICE)**

Internal combustion engines are heat engines that transform thermal energy from air-fuel mixture burning inside the combustion chamber into mechanical energy. Internal combustion engines can be divided into two ignition types which are spark ignition (SI) and compression ignition (CI).

Petrol engines, also known as SI engines, work according to the constant volume heat addition cycle (Otto cycle). A spark plug is used in the combustion process in SI engines, which helps ignite the compressed air-fuel mixture in the chamber. Petrol is used in SI engines as the working oil. In SI engines, air-fuel is combined and utilised in the suction stroke, which has a lower compression ratio hence there is generally lower thermal efficiency in SI engines compared to CI. However, heat transfer correlations obtained in SI engines are not applicable to that of CI engines due to radically different combustion characteristics in these two types of ICE. [11]

Diesel engines, commonly known as CI engines, are in high demand due to low emission levels and high thermal efficiency in comparison to SI engines [12], [13]. CI engines function based on Diesel cycle where heat is added in a fixed pressure cycle. Self-ignition is a key characteristic in CI engines because of the excessively compressed air that generates high temperature. CI engine uses diesel as its working fuel. Diesel fuel has a self-ignition temperature that is generally low and its nature is not volatile. A diesel injector is used to directly inject diesel at high pressure into the combustion cylinder. Compression ratio is generally higher in CI engines. CI engines possess low speed and high peak pressures. They also have the ability to function with diverse types of fuels such as biodiesel, standard diesel fuel, vegetable oils and heavy fuel oils.

## 2.5 Dual Fuel Engine Process and Applications

CI engines can either be operated in full load (100%) diesel or by using a dual fuel system, which incorporates gaseous fuels such as natural gas, landfill gas, syngas and biogas. Dual fuel engine is the type of CI engine proposed for this project.

Dual fuel CI engine utilises a premixed air-gas mixture of fuel that is ignited by an atomized liquid (pilot) fuel injection during the compression stroke inside the cylinder. Nevertheless, when a dual fuel engine operates at high replacement partial load, the thermal efficiency is lower than diesel engines [14]. Biogas (gaseous fuel) induction, the primary fuel, has the ability to decrease diesel (pilot fuel) consumption at substitution level to generate electricity that increases premixed combustion and reduces harmful emissions such as nitrogen oxide and particulate matter. Biogas has a high self-ignition temperature [12], which is compatible in a dual fuel CI engine.

This four-stroke CI dual fuel engine [10] operates by inducting biogas with air from intake manifold into the cylinder during intake stroke, TDC to BDC then the intake valves closes while the piston moves back towards the TDC as it compresses the biogas-air mixture to elevated temperatures and pressures. Ignition occurs when pilot fuel is sprayed by the injector into the cylinder. The combustion then exerts a downward force towards the piston at high pressure, known as the power stroke. Eventually, the exhaust valves open, the piston comes back to TDC and the exhaust stroke expels all the exhaust gases out of the combustion chamber. Thereafter, the cycle is repeated in a loop. Figure 2.3 and 2.4 shows the cross section of dual fuel CI engine and the setup of a dual fuel engine, respectively.

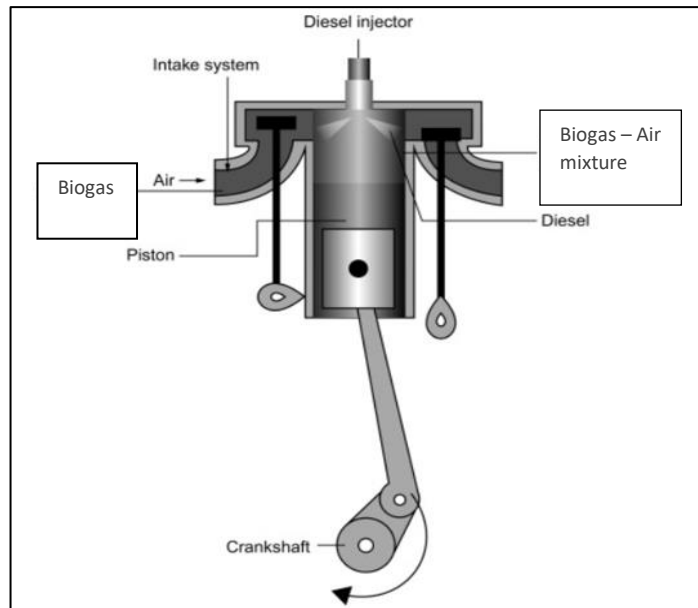


FIGURE 2.3 : Cross section of Dual Fuel CI Engine [15]

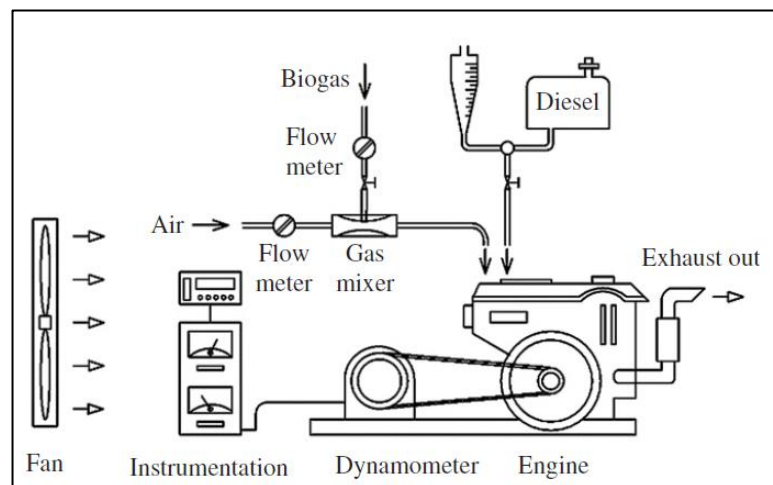


FIGURE 2.4 : Dual Fuel CI Engine Setup [16]

For adequate ignition, the diesel fuel amount required usually ranges between 10% to 20% of the actual amount needed for full load diesel fuel operation [9]. Biogas contribution ranging anywhere from 0% to 85% is able to replace a corresponding part of diesel fuel while the performance equals that of only diesel fuel operation [17]. To operate the engine at partial load, biogas supply needs to be reduced via a valve that controls gas. Air to fuel ratio is regulated by varying the flow rates of biogas injected into the external gas mixer. The performance and combustion characteristics of a dual-fuel engine varies with different compositions of biogas especially in its methane content.

Before biogas is channelled into the external gas mixer, it first has to be filtered [18] in a condensation trap and gas treatment unit in order to remove moisture and corrosive sulphur compounds. A governor controls the amount of diesel to be pumped into the combustion chamber for the dual fuel engine. When the gaseous fuel is supplied to the engine, the governor will slow down the amount of atomized diesel injected for combustion and this will cause the engine to run simultaneously with two fuels. CI engines are used as sources of stationary and motive power across the globe.

## **2.6 CFD Simulation**

Many researchers [18], [19], [20] applied Computational Fluid Dynamics (CFD) to simulate combustion in IC Engines due to modern computers that hold tremendous computational power. CFD is widely used across multiple applications utilising engine design, research and development because of its effective cost and time reduction as compared to conventional prototypes. CFD analysis is usually conducted using the ANSYS Software. However, their legacy IC Engine package requires high level of expertise and consumes a lot of time in completing the simulation runs.

ANSYS Forte [21] accelerates the IC engine simulation and can predict compression ignition engine performance in dual fuel modes as it has 65 validated fuel components. Hence, Forte helps engineers to create rapid designs of engines with high efficiency, cleaner burning, durability and fuel flexibility. Forte has an interface which is intuitive and user friendly. Forte's automatic mesh generation feature coupled with its robust capabilities for combustion modelling makes it very easy and quick to capture the in-cylinder physics. Forte incorporates the proven CHEMKIN-Pro solver technology which accurately predicts ignition, fuel effects and emissions by simulating surface chemistry and gas phase with comprehensive spray dynamics. Forte's chemistry solver contains dynamic adaptive chemistry and dynamic cell clustering which decreases the quantity of active species during simulation hence providing practical run times for usage of detailed chemistry.

## Summary

Many researchers [12], [13], [16], have suggested the use of gaseous fuels to partially replace diesel fuel among the various efforts to reduce diesel CI engine pollutant emissions. Korten [22] discovered that gaseous fuels such as biogas hold a very high potential as alternative fuels for diesel engines. Similarly, Mustafi [23] also claimed that diesel engines are highly compatible with low energy-content alternative fuels such as biogas. In spite of that, comparatively minimal research work on biogas–diesel dual fuel engines are discovered. Combustion characteristics, performances and exhaust emission analyses were performed by various research papers [19], [20] for a biogas–diesel dual fuel engine. However, their findings are mainly limited to conditions of low load or part load. Mustafi and Raine [23] analysed dual fuel engine emissions with natural gas and biogas but combustion characteristics in dual fuel mode were not presented in their research paper. Recent efforts using biogas–biodiesel in dual fuel application were found in [12], [14] with biogas application in a Homogeneous Charge CI engine; where engine performance, combustion and emission characteristics are thoroughly investigated. Researchers [13], [15], [19] have been posed serious questions about the future of CI engines in the face of extremely stringent greenhouse gas regulation and demand for fossil fuels. Thus, the proposed dual fuel engine in this project is a prominent step forward in the evolution of CI engines. This will help satisfy current and future market demands as well as environmental sustainability in the palm oil industry.

## **CHAPTER 3 : METHODOLOGY**

### **3.1 Research Methodology**

#### **3.1.1 Collection of Data**

Raw industrial data from October to November 2019 was collected from IOI Pukin Palm Oil Mill located in Rompin, Pahang. All required information collected is with the consented agreement of the mill management to execute this project. The data collection process was facilitated by the mill engineers in Pukin Mill. Majority of the data obtained for this project study is possessed from the power generation station and biogas recovery plant of Pukin Mill. The data gathered includes technical specifications of the 648kW diesel generator set, running hours, diesel consumption, biogas flowrate to boiler based on gas totalizer and biogas flowrate for open flaring in combustion chamber.

This project began with reviewing some previous studies and research works which are related to renewable energy for electricity generation. There are many methods for electricity generation from renewable resources but for this project, the focus will be on utilisation of biogas in dual fuel engines as this idea will be proposed to be incorporated in a 648kW diesel engine in PPOM.

#### **3.1.2 Analysis of Data**

Secondly, in the data analysis stage, key findings are structured based on the collected data by filtering big amounts of data through averaging process. In this process, the data was explored and scrutinized to discover patterns in it for hypothesis as well as to classify data into qualitative and quantitative categories. Data analysis provides a meaningful base to critical decisions to be made in this project. After extensive research on various credible academic journals mainly in the data analysis stage, six significant previous studies discovered that the maximum substitution level in (biogas-diesel) dual fuel engines ranges from 70-85% at intermediate loads [12], [23]. Their respective findings summarize that maximum diesel fuel displacement is limited by dual fuel engine stability and knocking. However, many researchers found that there are still limited strategies to enhance the operation of dual fuel engines at

part load and there is potential for higher substitution level of diesel with biogas. In the subsequent simulation methodology, the key procedures were obtained from the International Journal of Engineering Science and Technology (IJEST) research papers [18], [19] which present the CFD analysis of combustion and exhaust emissions in dual fuel CI engines.

### **3.1.3 Simulation using ANSYS Forte IC Engine software**

ANSYS is a computational fluid dynamics (CFD) software which utilises computer simulation that helps to save time and cost. The paramount of this project's execution lies in the ANSYS Forte IC Engine software where its functionality and features are leveraged to conduct biogas simulation into the proposed dual fuel engine. ANSYS Forte enables users to solve internal combustion engine problems related to fluid statics and dynamics by modelling and simulating surface chemistry and gas phase in the combustion chamber. In university research labs, the use of large, costly physical testing equipment (such as wind tunnels) is substituted by this powerful virtual simulation tool due to its high accuracy and reliability.

A project flow was constructed across both Final Year Project semesters and is supported by project planning made in the Gantt Charts thereafter. The project flow is strategically created to lock the scope in order to complete this project feasibly within the given time period. The project flow also describes and places a great emphasis on major tasks to be accomplished from the simulation study in a subsequent fashion. The project flow generally encompasses the three main components of a simulation study which are: pre-processor, solver and post-processor. In the project flow, there is a critical decision making step as a major course of action in the event of this project's success or failure. The project flow is illustrated in Figure 3.1



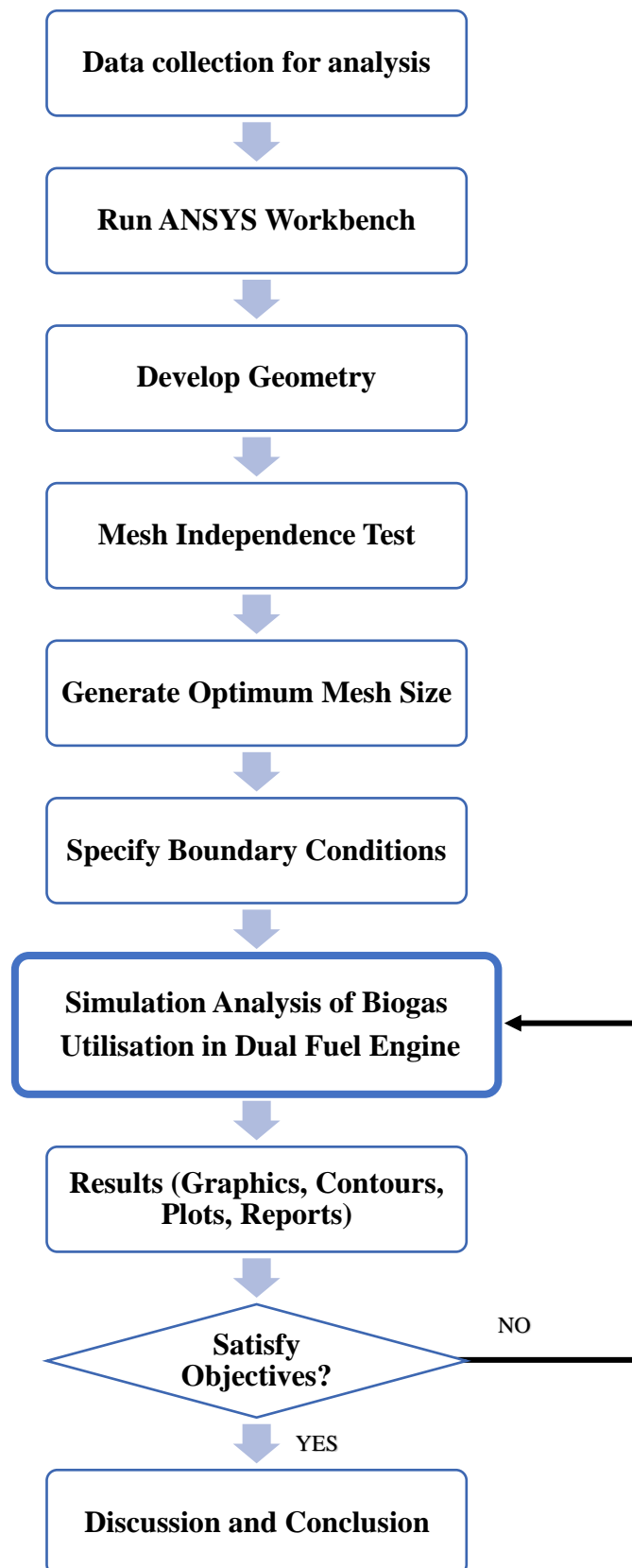


FIGURE 3.1 : Project Flow

### 3.2 Engine Specifications

The operating conditions, model and specifications of the existing generator-set diesel engine in PPOM obtained from the manufacturer catalogue [24] are presented in the following Table 3.1:

TABLE 3.1: Gen-set Specifications [24]

Engine type	Caterpillar PRIME 648ekW 810kVA (4-stroke cycle, water-cooled diesel)
Governor type	PEEC- Cat Electronic
Number of Cylinders	12 (V-configuration)
Rated Output Power	648kW
Displacement (per cylinder)	2439cc
Bore x Stroke	165.1mm x 137.16mm
Connecting rod length	26.16mm
Speed	1500rpm
IVC (°ATDC)	-95 degrees
EVO (°ATDC)	130 degrees
Power factor	0.8
Compression Ratio	16:1

### 3.3 Engine Performance Analysis

Several parameters will be employed to analyse the measured data. The engine performance analysis will be conducted using brake thermal efficiency, output power, specific fuel consumption and diesel displacement ratio for six different biogas-diesel compositions. For calculations, a constant value for pilot diesel fuel was maintained whereas adjustment to the engine output power was made through the varying biogas mass flow rates. To present the brake thermal efficiency, the following expressions from Tippayawong [16] were adopted:

For full load diesel operation,

$$\eta = \frac{W}{\dot{m}_{\text{diesel}} H_{\text{diesel}}}$$

For dual-fuel operation,

$$\eta = \frac{W}{\dot{m}^{\text{dual}}H^{\text{diesel}} + \dot{m}^{\text{biogas}}H^{\text{biogas}}}$$

Specific fuel consumption  $f_s$  [kg/kWh] represents the amount of fuel (in kilograms) required to produce 1kWh of electrical energy and is calculated for CI engine:

In full load diesel operation,

$$f_s = \frac{\dot{m}^{\text{diesel}}}{W}$$

In dual fuel operation,

$$f_s = \frac{\dot{m}^{\text{dual}} + \dot{m}^{\text{biogas}}}{W}$$

Diesel displacement ratio [ $r$ ], a measure of biogas substitution, is calculated by:

$$r = \frac{\dot{m}^{\text{diesel}} - \dot{m}^{\text{dual}}}{\dot{m}^{\text{diesel}}} \times 100\%$$

### 3.4 Steps Required for In-Cylinder Engine Simulation on ANSYS Forte

#### 3.4.1 Developing Geometry

A 60-degree sector mesh (1/6 of the cylinder) was selected to represent the entire geometry because the cylinder symmetry and periodicity of the injector nozzle-hole pattern can be taken advantage of. The sector mesh was used as the computational domain in the combustion chamber to reduce computational time so that this project can be feasibly completed within the given period. The 60-degree sector mesh was generated using the Sector Mesh Generator tool which adopts body fitted mesh calculations. Figure 3.2 illustrates the sector mesh geometry visualized in Forte's Ensign View:

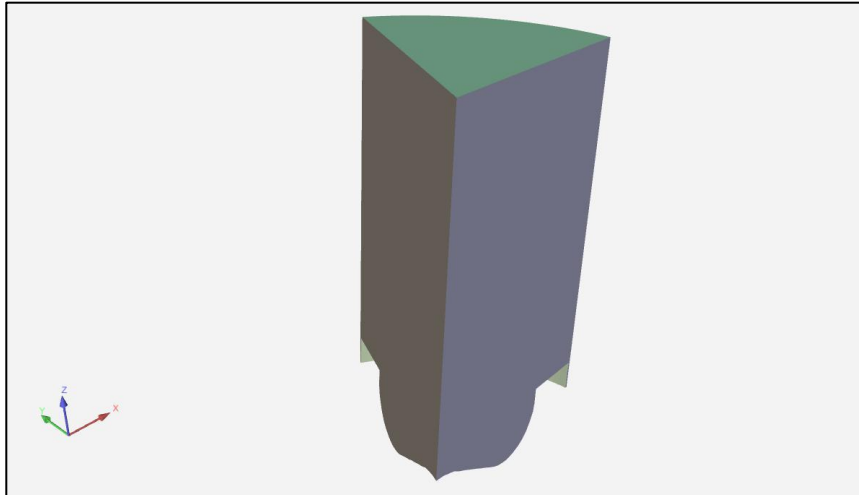


FIGURE 3.2 : Sector Mesh geometry from Enight

### 3.4.2 Generating Mesh

The KIVA-3V formatted body fitted mesh was utilised directly in the simulation. The body fitted mesh enables automatic decomposition of the geometric model into specific bodies and volumes in order to create a suitable mesh on the bodies whereby the mesh deformation was allowed when the body deforms.

Conventionally, in the meshing component, a grid independence test is to be performed for manually created mesh to reach independence in which further refining the mesh size does not significantly affect the solution obtained. This procedure usually takes a long time. However, due to the advanced features of solution adaptive mesh refinement in ANSYS Forte, the mesh independence study was quickly completed. For the mesh generation, the base element size was determined by the mesh independency investigation that provides high accuracy and stability as well as lowest computational time. A fine resolution of the sector mesh was resolved in the azimuthal direction. However, there was coarse mesh resolution in the z- and r-directions. Figure 3.3 illustrates the KIVA-3V sector mesh visualized in Forte's Simulate 3-D View:

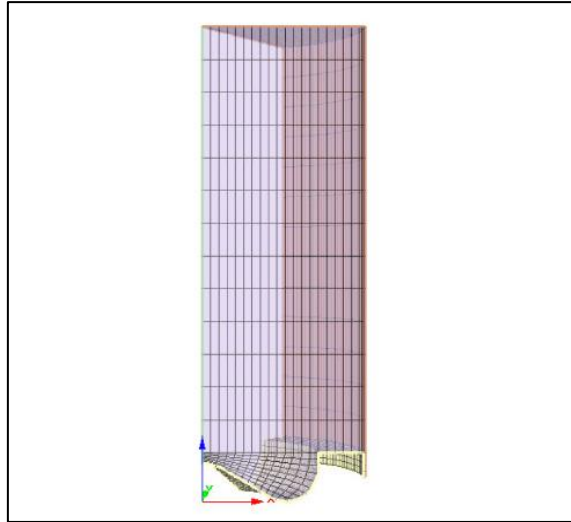


FIGURE 3.3 : 60-degree KIVA-sector mesh

### 3.4.3 Boundary Conditions

The main four zones [20] under the boundary conditions were piston, head, liner and injector as illustrated in Figure 3.4.

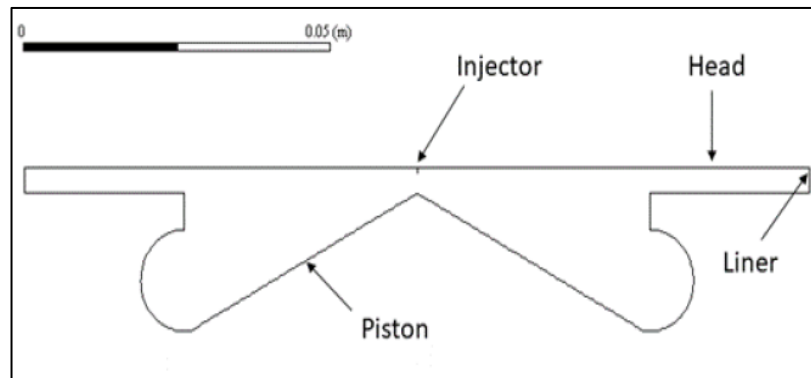


FIGURE 3.4: Combustion Chamber 2D-view at TDC [20]

As the injector nozzle diameter size was not specified in the manufacturer's catalogue [24], diesel was injected through a standard 0.15mm diameter nozzle [19]. Initialization parameters such as x,y,z coordinates, injection profile, initial turbulence, swirl profile were setup according to their default parameters.

### 3.4.4 Solver Setup and Models Used

The solver and models options were set up using guided tasks in the Forte simulation workflow tree. In many cases, default parameters are assumed and employed, such that no input is required. The required inputs and changes to the setup panels for a particular case were described in the Forte tutorial file [21] entitled

“Simulating Dual Fuel Combustion”. For turbulence analysis, RNG  $k-\varepsilon$  model was used. In terms of chemistry model, a pre-installed chemistry set that comes together with Forte was employed. This chemistry-set file (.cks) is a standard CHEMKIN file [21] which is a reduced mechanism specifically for dual-fuel conditions. The automatic time step control algorithm by Forte determined the actual local time steps to run simulation.

A solid-cone spray model with droplet-breakup was employed for spray injection governed by KH-RT sub-models. [26, 27]. For spray injection, the radius of influence collision model [28] was also utilised. Vaporization properties for each surrogate component is also taken into account using a discrete multi-component spray-vaporization model [29]. For these models mentioned, default parameters were used. To solve all chemical species equations included in the detailed kinetics mechanism, via CFD calculations, an-operator splitting method is used.

### **3.4.5 Simulation Analysis**

Heat transfer analysis [18] for engine combustion characteristics will be performed in ANSYS Forte IC Engine simulation. Under this analysis, contour results of multiple combustion parameters such as in-cylinder temperature distribution and peak pressure will be obtained at various biogas-diesel mass flow rates. Moreover, this analysis will also yield results of chemical rate of heat release (RoHR) and brake thermal efficiency at different primary and pilot fuel compositions. This analysis will also present results of the mixing, transport and reaction of chemical species which changes with time. This CFD model solves conservation equations encompassing convection, diffusion, and reaction sources for individual component species. Atomized (gas) phase of diesel modeled as n-heptane due to a cetane number similar to diesel fuel. Biogas-air modeled as a mixture of methane, carbon dioxide, oxygen and water. Therefore, the ultimate goal of this CFD simulation is to analyse the effect of six different biogas-diesel compositions on combustion parameters for a fixed engine load.

### 3.4.6 Simulation Procedure

The procedure for combustion simulation analysis will be performed from intake valve closed (IVC) to exhaust valve open (EVO) through different operating modes. The biogas mass flow rates will be adjusted according to pilot diesel fuel supply. The biogas will be inducted together with the air during intake stroke of the engine at five different flow rates. Hence the biogas (primary fuel) will be decreased from 85% to 60% (by volume) with a decremental step of 5% while diesel (pilot fuel) will be simultaneously increased from 15% to 40% with incremental step of 5%. The load level (power percentage) will be set at 75% of 648kW which is 486kW while the engine is operated at constant speed of 1500rpm, corresponding to 50 Hz. Using the output parameters obtained from simulation analysis, the effect of variation is will be studied in detail using resulting contours and graphs. Table 3.2 shows the general procedure for simulation analysis.

TABLE 3.2: General Procedure for Simulation Analysis

Biogas	Diesel	Engine Load Levels
85%	15%	486kW (75%)
80%	20%	
75%	25%	
70%	30%	
65%	35%	
60%	40%	
<b>Output Parameters (Expected Results)</b>		
Peak Pressure, Temperature Distribution Profile, Rate of Heat Release (ROHR), Crank Angles, Emission Rates		

### 3.5 Project Planning









Project planning for FYP I and FYP II was conducted with the aid of Gantt charts in Figure 3.5 and 3.6 accompanied by milestones in Table 3.3 and 3.4 consisting of research works, discussions, methodology formulations, submissions, presentations and milestones for important task executions to feasibly complete this project in a time span of 14 weeks each semester.

Task	Week													
	1	2	3	4	5	6	7	8	9	10	11	12	13	14
Project Title Confirmation and Project Discussion with SV	★													
Identification of Scope of Study					○									
Critical Literature Review on Related Topic														
Progress Report 1						★								
Determining Critical factors and Output Parameters for Simulation Study						○								
Preparation of Proposal Defence										★				
Familiarizing with ANSYS software												○		
Progress Report 2 and Preparation for interim report												★		
Submission of Interim Report														★

FIGURE 3.5: Gantt Chart FYP I



TABLE 3.3: Milestones (FYP I)

Week	FYP Markers	FYP I Activities
1		Title Selection and Confirmation
6		Progress Report 1 Submission
10		Proposal defense
12		Progress Report 2 Submission
14		Interim Report Submission
Week	Project Markers	FYP I Activities
5		Locking scope of study according to feasibility to complete within given time frame
6		Determining critical factors and output parameters for simulation study in ANSYS Forte
12		Familiarizing with ANSYS software by undergoing academic lab sessions

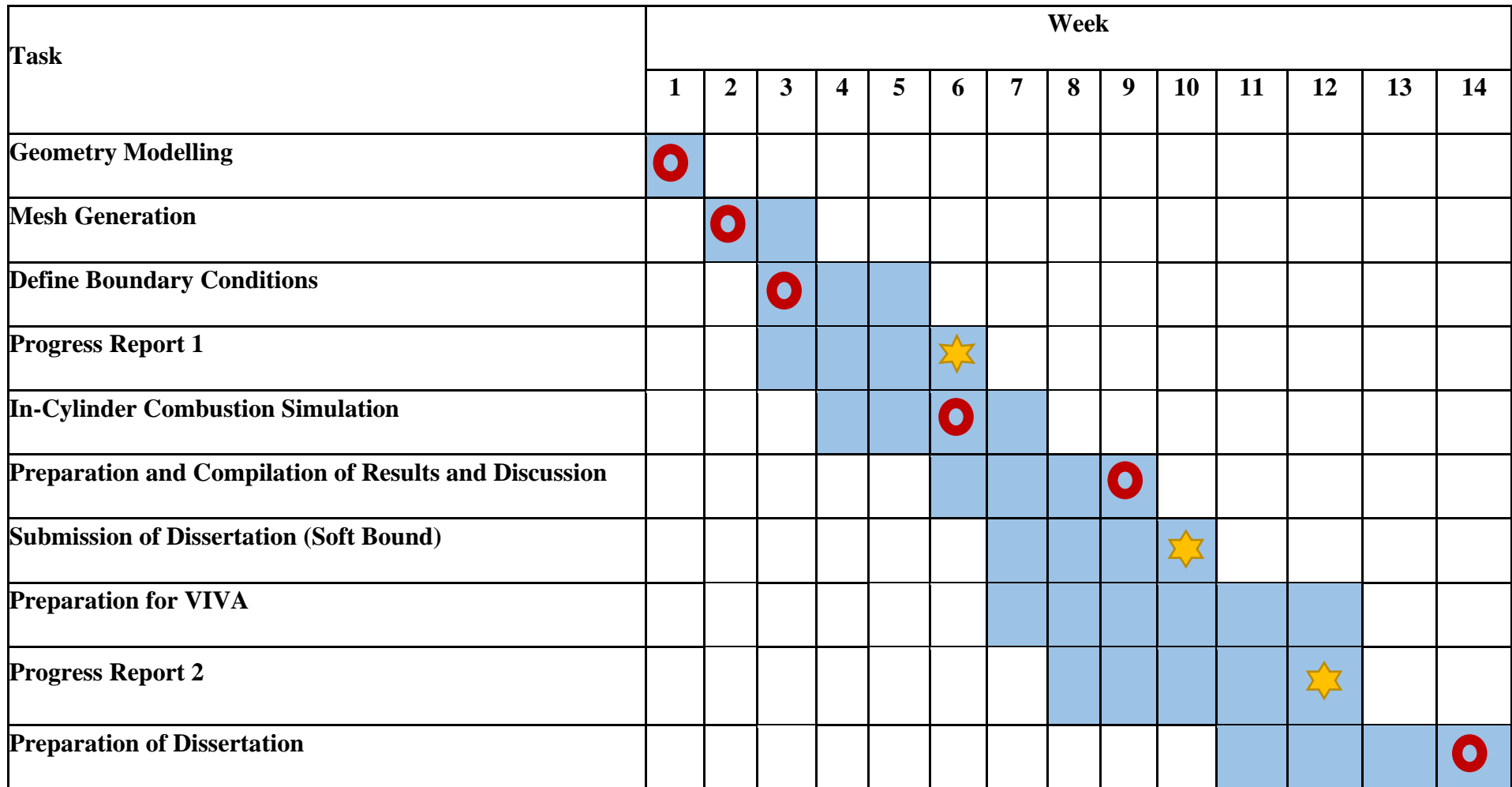


FIGURE 3.6: Gantt Chart FYP II

TABLE 3.4: Milestones (FYP II)

Week	FYP Markers	FYP II Activities
6	★	Progress Report 1 Submission
10	★	Submission of Dissertation (Soft Bound)
12	★	Progress Report 2 Submission and Completion of VIVA
Week	Project Markers	FYP II Activities
1	○	Geometry Modelling of Sector Mesh
2	○	Mesh Independence Test (Optimum Mesh Size Determination)
3	○	Boundary Conditions Specifications of Relevant Properties, Reactions and Zones
6	○	In-Cylinder Combustion Simulation of Dual Fuel Engine to study Combustion Characteristics between Biogas-Air Mixture and Diesel Fuel
9	○	Compilation of Results and Discussion
14	○	Completion and Submission of Hard Bound Dissertation

## **Summary**

The research methodology and project planning is strategically designed for the timely completion and effective execution of the simulation study. The simulation study was carried out as per the project flow using ANSYS software available in the Block 17 CFD laboratory of Universiti Teknologi PETRONAS. The simulation study first began by determining the input parameters in the combustion reaction. Thereafter, the in-cylinder simulation analysis was carried out using the tabulated simulation experiments which closely relate to the research work of Hussain [18], [19] . The aim of the simulation experiment is to determine the maximum amount of biogas that can displace diesel, at the same time ensure high engine stability and performance. For each set of experiment, results such as contours and graphs for the output parameters and expected results were critically analysed and discussed. In the event that the goals of this project are not met, the simulation study will be repeated to rectify the problems and challenges faced.

## CHAPTER 4 : RESULTS AND DISCUSSION

### 4.1 Overview

This chapter will first describe how a mesh independent solution was obtained for CFD simulation. Thereafter, the basis of calculation made to extract input values and facilitate calculation of engine performance parameters is presented where comparisons between actual and theoretical results are plotted and interpreted. A sample calculation is also provided to demonstrate the working steps to arrive at the performance parameters output values based on formulas provided in chapter 3.3. In this chapter, the effect of engine load and six different biogas-diesel compositions on a dual-fuel engine is discussed. Lastly, the CFD simulation results of heat transfer analysis as well as in-cylinder combustion and exhaust emission characteristics of a dual-fuel CI engine are mainly illustrated by contours, thereafter plotted in graphs and thoroughly discussed.

### 4.2. Mesh Independence Test

A mesh independence test was performed with three different mesh resolutions to identify how it affects the sensitivity of results. Initially, the mesh had 12780 cells at IVC. For comparison, the coarse mesh results were compared to that of medium and fine mesh which had 24682 and 48030 cells, respectively at IVC. The results of peak pressure acquired and computational time with the variation in the number of cells is tabulated in Table 4.1.

TABLE 4.1: Results from Mesh Independence Test

<b>Mesh Resolution</b>	<b>Fine</b>	<b>Medium</b>	<b>Coarse</b>
Element Size (mm)	1.6	2	2.5
Number of cells (at IVC)	48030	24682	12780
Simulation Run Time (hours)	8.5	4.9	3.1
Peak Pressure (MPa)	3.738	3.732	3.729

Based on the results obtained in Table 4.1, it can be observed that the solution of peak pressure does not change significantly with further mesh refinement.

Therefore, to check for a mesh independent solution, a graph of peak pressure against number of cells (at IVC) was plotted in Figure 4.1.

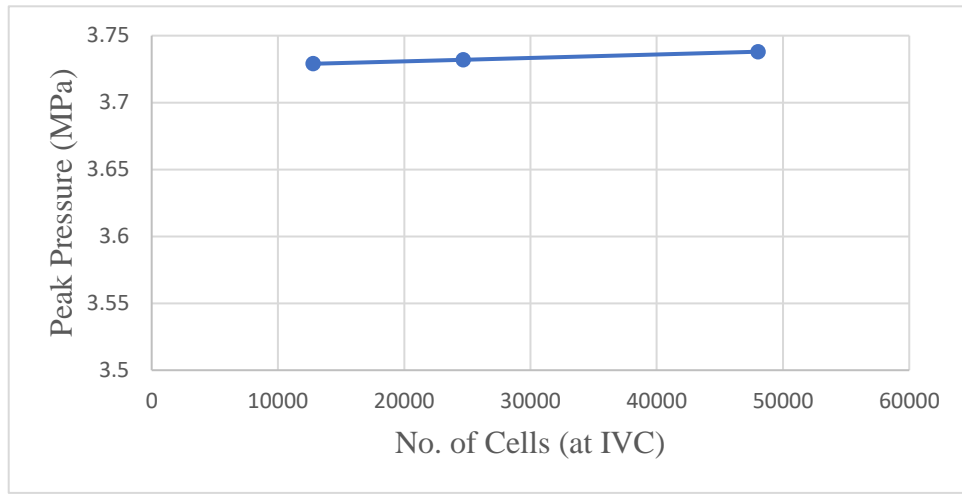


FIGURE 4.1: Mesh Independent Solution Graph

The results using all three mesh resolutions were quite similar, with peak pressure within 3.729-3.738 MPa for the cases modelled. It's been observed that when the mesh is refined further from 12780 cells to 24682 cells, the jump in value for peak pressure is not significant. This is mainly due to the advanced adaptive mesh refinement feature in Forte. The same observation applies to a fine mesh (48030 cells) which consumes an additional 5.4 hours for simulation. Therefore, this indicates that a solution value independent of mesh resolution has been reached at 12780 cells. Hence, the coarse mesh was used for all the remaining simulations reported. The computational time for the simulation with the coarse mesh was approximately 3 hours on a dual Intel® Core™ i7-8550U CPU (2 total cores).

### 4.3 Basis of Calculation

TABLE 4.2: Data for Key Parameters used in Engine Calculations

Item	Descriptions	Estimated Value
1	Caterpillar PRIME Diesel Gen-Set Capacity	684kW 486kW (at 75% load)
2	Average power factor	0.8

3	Dual Fuel CI Engine efficiency ( $\eta$ )	Min = 17% Avg = 20% Max = 23%
4	Heating value of diesel	43 MJ/kg
5	Heating value of biogas	24.5 MJ/kg
6	Density of diesel	830 kg/ m <sup>3</sup>
7	Density of biogas	1.1 kg/m <sup>3</sup>

The data shown in Table 4.2 will be utilised for calculating significant combustion parameters such as brake thermal efficiency, specific fuel consumption and diesel displacement ratio.

Based on calculations obtained from biogas commissioning project reports by CH Environment Sdn.Bhd, **1 MW engine output power requires 500 m<sup>3</sup>/hr biogas.**

$\therefore$  Combustion biogas inlet flow rate @ 75% load (486kW) = **243 m<sup>3</sup>/hr = 0.0675 m<sup>3</sup>/s**

Combustion air inlet flow rate = **48.8 m<sup>3</sup>/min = 0.813 m<sup>3</sup>/s**

TABLE 4.3: Theoretical Diesel Consumption for 648kW Gen Set (PPOM)

<b>Theoretical Diesel Consumption</b>	
100% load with fan	171.7 L/hr
75% load with fan	130.4 L/hr

The data presented in Table 4.3 was provided by the mill management which was partly extracted from the manufacturer catalogue [24]. Intermediate engine load of 75% was selected as the calculations [16] require the pilot diesel fuel amount to be constant at a specified load. Therefore, the following conversion was made:

Theoretical Diesel consumption @ 75% load (486kW)

= **130.4L/hr = 2.17 L/min = 3.62 x 10<sup>-5</sup> m<sup>3</sup>/s**

TABLE 4.4: Actual Diesel Consumption for 648kW Gen Set (PPOM)

<b>Oct 2019 (Day)</b>	<b>Diesel usage (L)</b>	<b>Total RIH (hr)</b>	<b>Diesel Usage Rate (L/hr)</b>	<b>Nov 2019 (Day)</b>	<b>Diesel usage (L)</b>	<b>Total RIH (hr)</b>	<b>Diesel Usage Rate (L/hr)</b>
2	579	3	193	1	799	4	199.71
4	818	4	204.5	4	431	2	215.5
6	736	4	184	5	1147	6	191.17
9	813	4	203.25	8	830	4	207.5
11	643	3	214.33	12	480	2	240
13	1138	6	189.67	15	777	4	194.25
16	466	2	233	18	698	3	232.67
18	845	4	211.25	19	452	2	226
20	1124	6	187.33	20	1402	6	233.67
23	672	3	224	22	1158	6	193
25	811	4	202.75	25	1431	6	238.5
27	1118	6	186.33	27	1069	5	213.8
30	431	2	215.5	30	1033	5	206.6
Average actual diesel consumption			<b>210.72 L/hr (100% load)</b>				
			<b>158.04 L/hr (75% load)</b>				

The data presented in Table 4.4 comprises of actual diesel consumption in the month of October and November 2019. Based on the data, the average actual diesel consumption was calculated and found to be 210.72 L/hr at full load. Since intermediate load was selected, the following calculation and conversion was made:

Actual Diesel consumption @ 75% load (486kW)

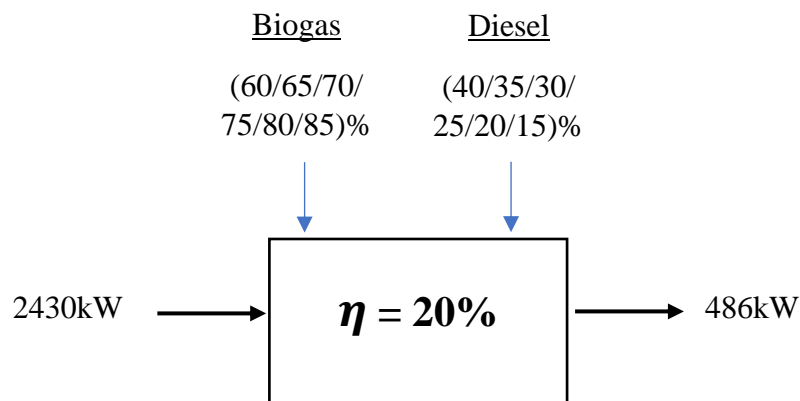
$$210.72 \text{ L/hr} \times 0.75 = 158.04 \text{ L/hr} = 2.63 \text{ L/min} = 4.39 \times 10^{-5} \text{ m}^3/\text{s}$$



#### 4.4 Engine Performance Analysis

The formulas provided in chapter 3.3 were used to compute values of Brake Thermal Efficiency (BTE). For comparison between theoretical and actual calculations of thermal efficiencies,  $\eta = 17\%$ ,  $20\%$  and  $23\%$  were considered, which are the minimum, average and maximum values in a dual fuel CI engine operation. The sample calculations are as follows:

At average BTE,  $\eta = 20\%$ ,



i) For a dual fuel engine with 60% biogas 40% diesel mix :

Theoretical calculation

$$W = 486\text{kW}$$

$$\dot{m}_{\text{dual(theor)}} = \dot{V}_{\text{dual(theor)}} \times \rho_{\text{diesel}} = (3.62 \times 10^{-5} \text{m}^3/\text{s} \times 830 \text{kg/m}^3) \times 40\% = 0.012 \text{kg/s}$$

$$H_{\text{diesel}} = 43000 \text{kJ/kg}$$

$$\dot{m}_{\text{biogas}} = \frac{\text{Engine power input } \left(\frac{\text{kJ}}{\text{s}}\right)}{H_{\text{biogas}}} = \frac{2430}{24500} = 0.099 \text{kg/s} \times 60\% = 0.0595 \text{kg/s}$$

$$H_{\text{biogas}} = 24500 \text{kJ/kg}$$

$$\eta \text{ (theor)} = \frac{486}{0.012(43000)+0.0595(24500)} = 0.2462 = \mathbf{24.62\%}$$

### Actual calculation

$$W = 486\text{kW}$$

$$\dot{m}_{\text{dual(actual)}} = \dot{V}_{\text{dual(actual)}} \times \rho_{\text{diesel}} = (4.39 \times 10^{-5} \text{m}^3/\text{s} \times 830 \text{kg/m}^3) \times 40\% = 0.0146 \text{kg/s}$$

$$H_{\text{diesel}} = 43000 \text{kJ/kg}$$

$$\dot{m}_{\text{biogas}} = \frac{\text{Engine power input } (\frac{\text{kJ}}{\text{s}})}{H_{\text{biogas}}} = \frac{2430}{24500} = 0.099 \text{kg/s} \times 60\% = 0.0595 \text{kg/s}$$

$$H_{\text{biogas}} = 24500 \text{kJ/kg}$$

$$\eta \text{ (actual)} = \frac{486}{0.0146(43000)+0.0595(24500)} = 0.233 = \mathbf{23.3\%}$$

The same calculation method (theoretical and actual) was repeated at BTE ( $\eta = 17\%$ ,  $\eta = 20\%$ ,  $\eta = 23\%$ ) for other compositions and the results obtained are tabulated in Table 4.5, 4.6 and 4.7:

TABLE 4.5: Theoretical and Actual BTE ( $\eta = 20\%$ )

Ratio (BG/diesel)	$\eta$ (theo)	$\eta$ (actual)
60/40	24.62%	23.32%
65/35	23.93%	22.85%
70/30	23.28%	22.39%
75/25	22.66%	21.95%
80/20	22.07%	21.53%
85/15	21.51%	21.13%

The results obtained in Table 4.5 were used to plot the graph of thermal efficiency versus biogas-diesel ratio at  $\eta = 20\%$  in Figure 4.2.

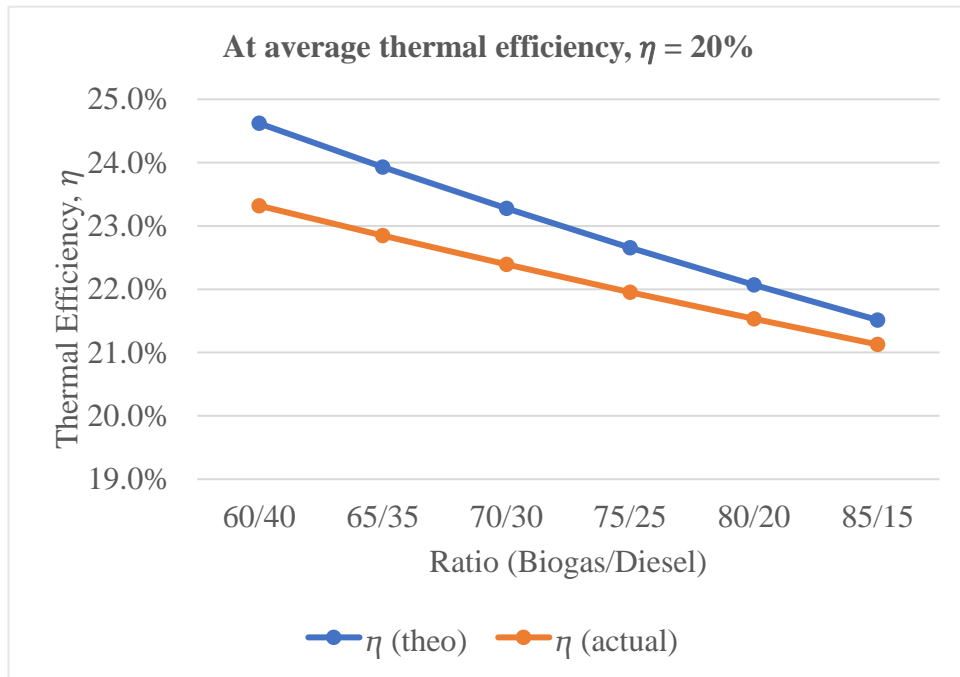


FIGURE 4.2: Theoretical and Actual BTE ( $\eta = 20\%$ )

Based on Figure 4.2, it is clear that the theoretical values of BTE are higher than actual BTE across all compositions. However, as the biogas substitution increases, the theoretical and actual BTE plots converge further which shows minimum difference can be achieved with lower diesel usage in the dual-fuel mix. To verify the interpretation, results for BTE at  $\eta = 17\%$  and  $\eta = 23\%$  were plotted and analysed.

At minimum BTE,  $\eta = 17\%$ ,

TABLE 4.6: Theoretical and Actual BTE ( $\eta = 17\%$ )

Ratio (BG/diesel)	$\eta$ (theo)	$\eta$ (actual)
60/40	21.78%	20.76%
65/35	21.04%	20.20%
70/30	20.35%	19.67%
75/25	19.70%	19.17%
80/20	19.10%	18.69%
85/15	18.52%	18.24%

The results obtained in Table 4.6 were used to plot the graph of thermal efficiency versus biogas-diesel ratio at  $\eta = 17\%$  in Figure 4.3.

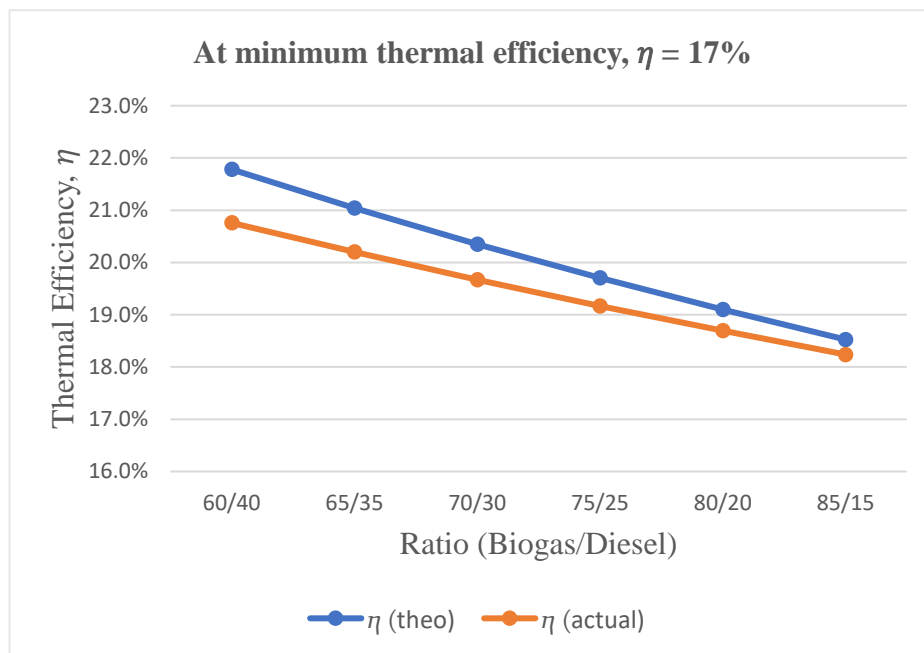


FIGURE 4.3: Theoretical and Actual BTE ( $\eta = 17\%$ )

Based on Figure 4.3, the minimum thermal efficiency also demonstrates the same trend where theoretical BTE is greater than actual BTE for all compositions. With more biogas substitution, convergence between plots also increases.

At maximum BTE,  $\eta = 23\%$ ,

TABLE 4.7: Theoretical and Actual BTE ( $\eta = 23\%$ )

Ratio (BG/diesel)	$\eta$ (theo)	$\eta$ (actual)
60/40	27.24%	25.66%
65/35	26.63%	25.30%
70/30	26.04%	24.94%
75/25	25.48%	24.59%
80/20	24.94%	24.26%
85/15	24.43%	23.93%

The results obtained in Table 4.7 were used to plot the graph of thermal efficiency versus biogas-diesel ratio at  $\eta = 23\%$  in Figure 4.4.

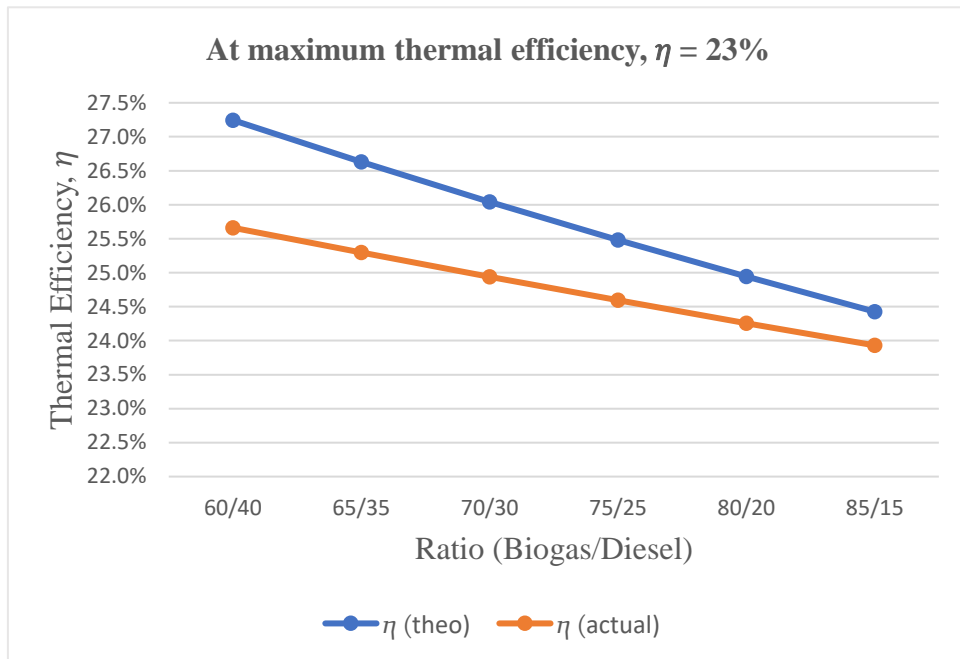


FIGURE 4.4: Theoretical and Actual BTE ( $\eta = 23\%$ )

Figure 4.4 confirms that even at maximum thermal efficiency, the similar conclusion can be drawn for all ranges of BTE. Conclusively, higher biogas substitution into the dual-fuel mix reduces the deviation between actual and theoretical values of thermal efficiency and provides higher accuracy.

## 4.5 Effect of engine load and biogas-diesel composition variations on CI engine operated in dual fuel mode

### 4.5.1 Brake Thermal Efficiency

The brake thermal efficiency of the present 648kW diesel generator against engine load at varying biogas-diesel compositions were theoretically calculated and the plotted results are presented in Figure 4.5.

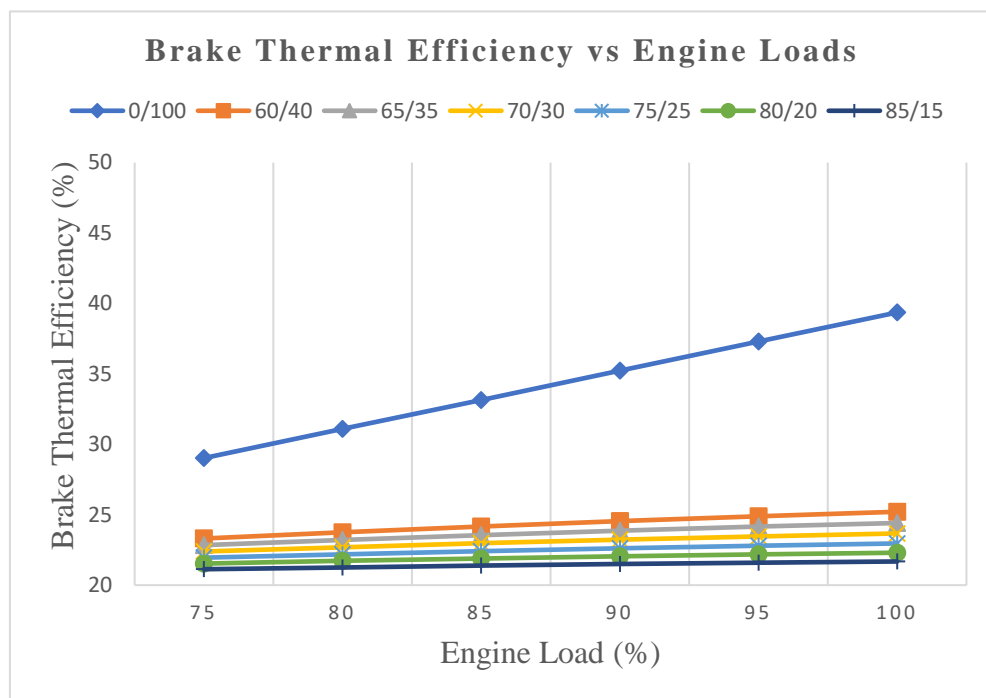


FIGURE 4.5: Brake thermal efficiency against engine loads (1500rpm constant)

It is observable that the brake thermal efficiency increases linearly with engine load for each biogas-diesel composition. Based on the figure, it can be seen that biogas substitution volume affects the brake thermal efficiency such that as the diesel displacement with biogas increases, the brake thermal efficiency decreases. The linear plot located at the top most of the graph is most conspicuous because a CI engine run with 100% diesel (full load) yields the highest brake thermal efficiency across all engine loads. This clearly illustrates that when pure diesel mode is compared to that of dual fuel modes, lower efficiencies will be obtained for dual-fuel operation regardless of engine load. It is therefore suggested to operate the diesel gen-set in dual-fuel mode at 75% engine load, where there is minimum difference in brake thermal efficiency as compared to pure diesel operation.

#### 4.5.2 Specific Fuel Consumption

Figure 4.6 illustrates the results of specific fuel consumption (*sfc*) versus engine load at different biogas-diesel compositions. The specific fuel consumption indicates the effectiveness of a power generation system for conversion of a certain fuel amount into electrical energy. Generally, the lower the *sfc*, the better it is.

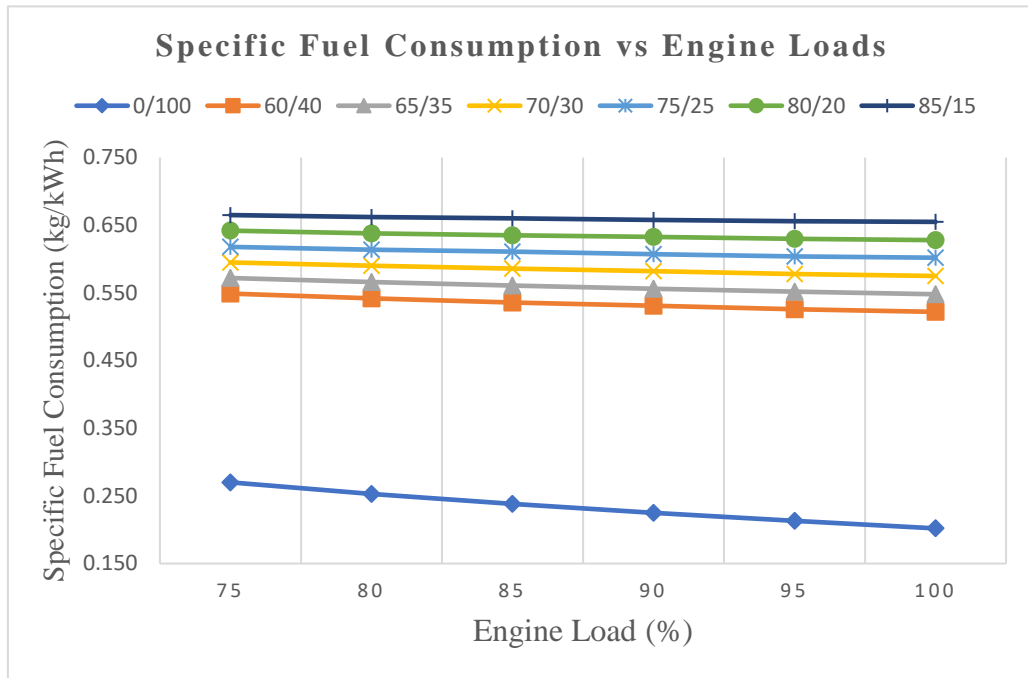


FIGURE 4.6: Specific fuel consumption against engine loads (1500rpm constant)

It can be seen that *sfc* decreases with increase in engine load for all cases. This proves that combustion process is better at increasing engine loads for the CI engine. The effect of variation in biogas-diesel mix to the *sfc* is illustrated in the graph. When the gen-set is operated in dual fuel mode, the *sfc* is higher compared to that of pure diesel mode. This is due to biogas-diesel mass flow rates added up which contributes to a higher volume of overall fuel (pilot and primary). Methane found in biogas is the most prominent component in combustion process due to its heat energy content. Therefore, when the gen-set is run in dual fuel mode, higher *sfc* is obtained as compared to that of pure diesel mode. More specifically, as the biogas substitution increases, the *sfc* increases. Hence, yet again it is recommended to run the gen-set in dual-fuel mode at 75% engine load, where there is minimum difference in specific fuel consumption as compared to full load diesel operation.

### 4.5.3 Diesel Replacement Ratio

The Diesel Replacement Ratio (DRR) versus engine loads of the gen-set for different biogas-diesel compositions is shown in Figure 4.7.

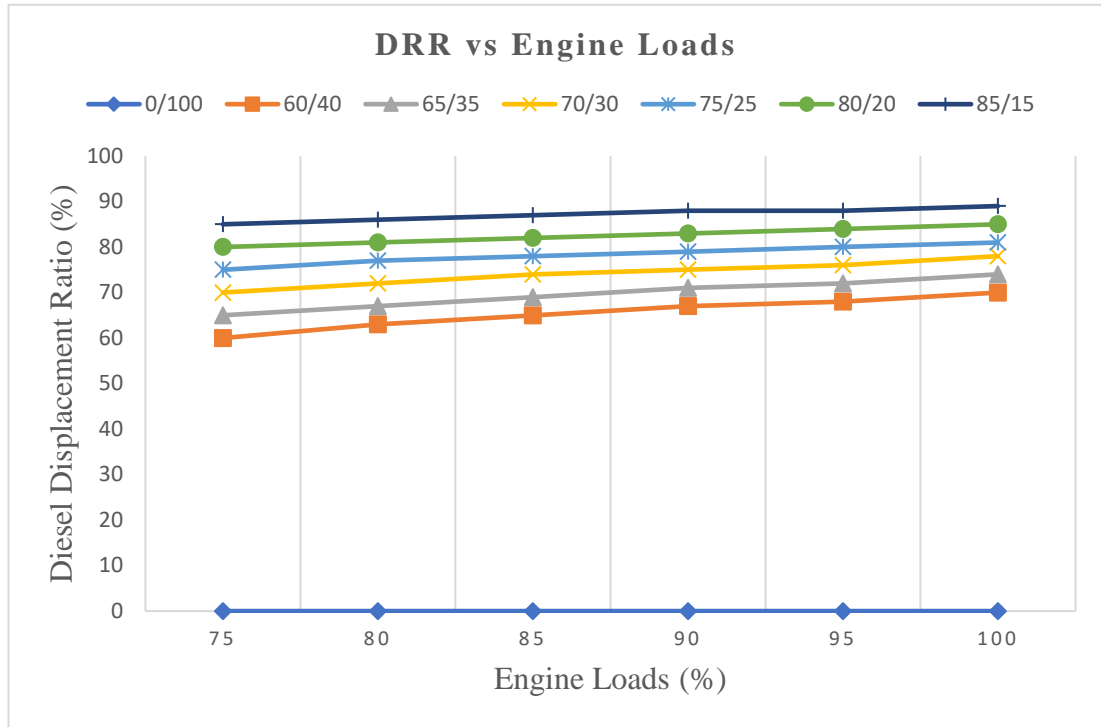


FIGURE 4.7: Diesel displacement ratio against engine loads (1500rpm constant)

The DRR is zero when the gen-set is operated fully using diesel without biogas substitution. The DRR varies for each biogas-diesel composition. Generally, the DRR increases as the engine load increases. As the biogas substitution increases, the DRR also increases across engine loads. A contrary suggestion can be drawn from this observation that the gen-set should be run in dual-fuel mode at 100% engine load instead where the diesel replacement ratio is maximum for all biogas-diesel compositions.



## 4.6 CFD Simulation Results of Heat Transfer Analysis and In-Cylinder Combustion and Exhaust Emission Characteristics in Dual Fuel CI Engine

CFD combustion simulation was conducted to study how six different levels of biogas substitution affects significant combustion parameters at 75% engine load and 16:1 compression ratio. Biogas substitution was varied from 60% to 85% after which the analysis of the variation effect was presented using contours and graphs.

### 4.6.1 Effect of Biogas substitution on Peak Pressure

Based on Figure 4.8(a) to 4.8(f), change in combustion peak pressure with percentage decrease in biogas is represented by contours at  $-5^\circ$  ATDC (power stroke). As biogas substitution in the mixture decreases the peak pressure becomes higher at intermediate loads. The main reason being, as biogas percentage in the mixture decreases, the ignition delay period reduces due to higher amount of injected diesel which leads to autoignition of the fuel and higher peak pressures. [25] Hence, these results can be validated against the range of peak pressure values obtained from the CFD analysis conducted by Hussain [19].

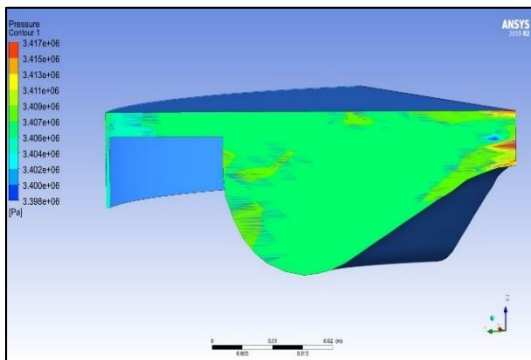


FIGURE 4.8(a): 85% biogas  
(3.417MPa)

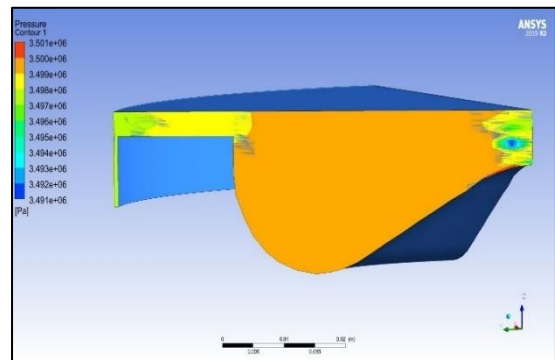


FIGURE 4.8(b): 80% biogas  
(3.501MPa)

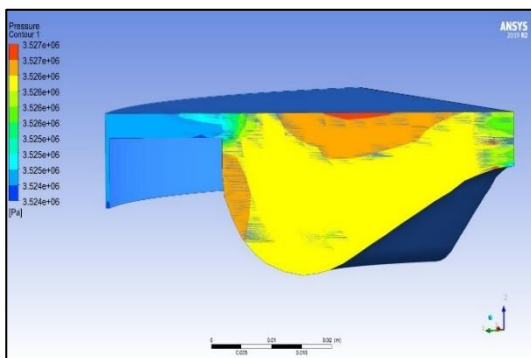


FIGURE 4.8(c): 75% biogas  
(3.527MPa)

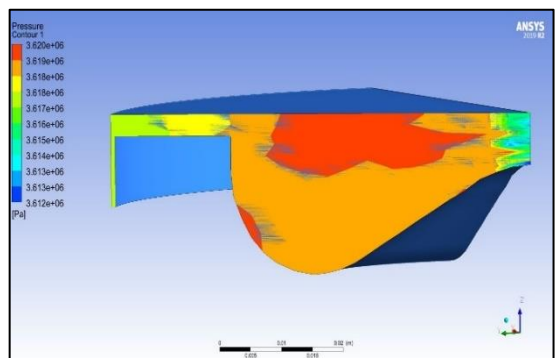


FIGURE 4.8(d): 70% biogas  
(3.62MPa)

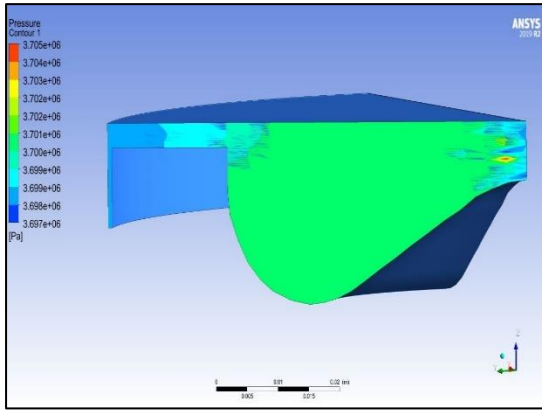


FIGURE 4.8(e): 65% biogas  
(3.705MPa)

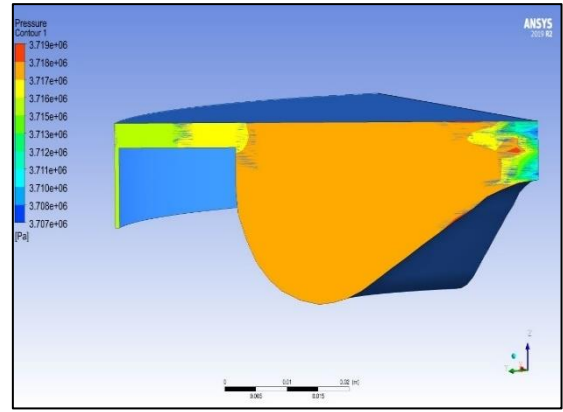


FIGURE 4.8(f): 60% biogas  
(3.72MPa)

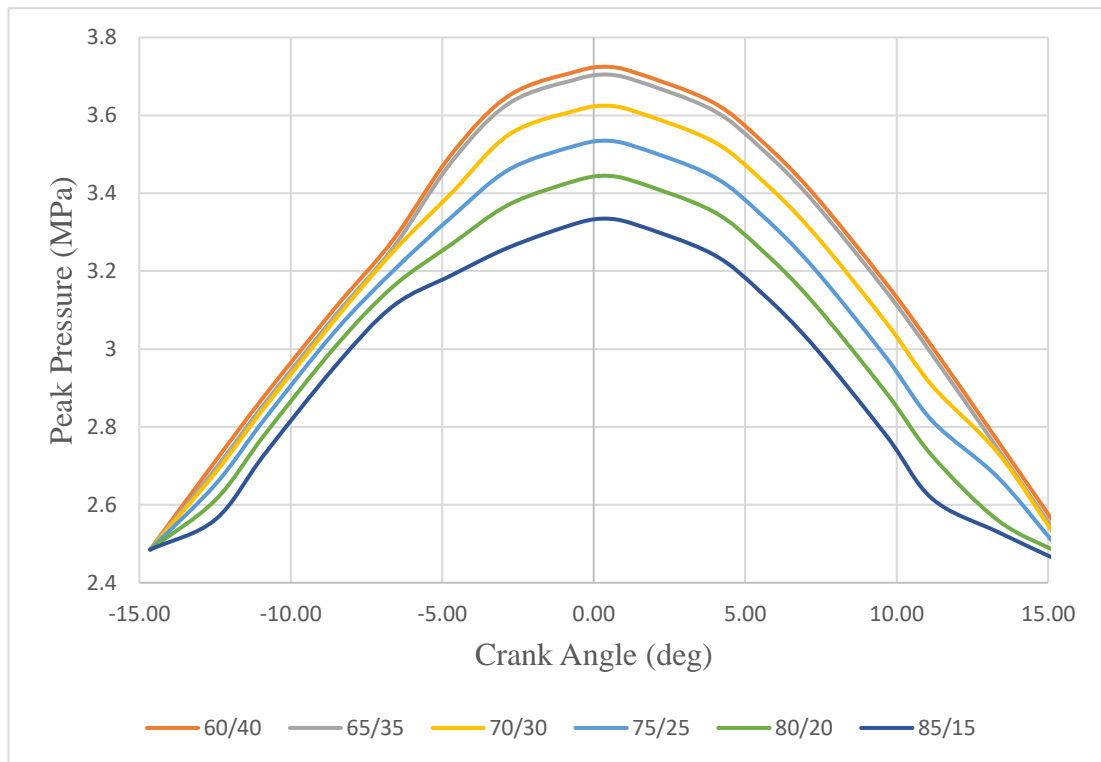


FIGURE 4.9: Pressure vs Crank Angle Diagram

Based on Figure 4.9, a very low difference in in-cylinder peak pressure is observed between the 60/40 and 63/35 mix. However, between 65/35mix to 80/20 mix, the deviation remains fairly the same. The peak pressure of 85/15 biogas-diesel shows the largest deviation between all compositions and has the lowest peak pressure amongst all.

#### 4.6.2 Effect of Biogas substitution on Maximum Temperature

Based on Figure 4.10(a) to 4.10(f), change in maximum combustion temperature with decrease in biogas substitution levels are represented by contours at 21 °ATDC (power stroke). As biogas substitution in the mixture decreases the maximum temperature becomes higher. The main reason is because lower biogas substitution levels yield greater total injected diesel mass into the combustion chamber hence causing a significant temperature rise and thereafter rapid combustion rates are obtained as more diesel is injected. Hence, these results can be validated using the ideal gas law  $PV=nRT$  which shows temperature is directly proportional to pressure in a closed exothermic reaction. Therefore, as the peak pressure increases, the maximum combustion temperature also increases with lower biogas substitution.

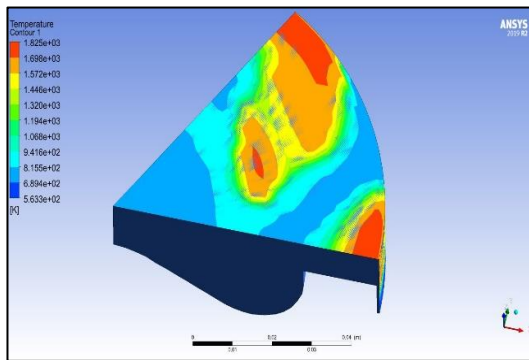


FIGURE 4.10(a): 85% biogas  
(1825K)

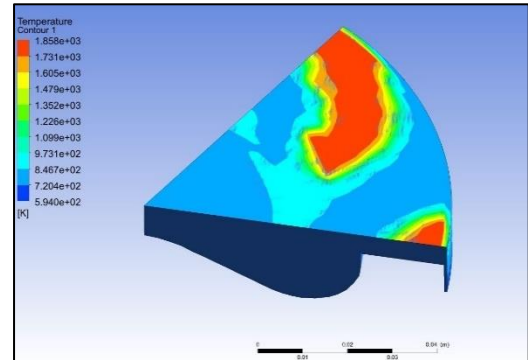


FIGURE 4.10(b): 80% biogas  
(1858K)

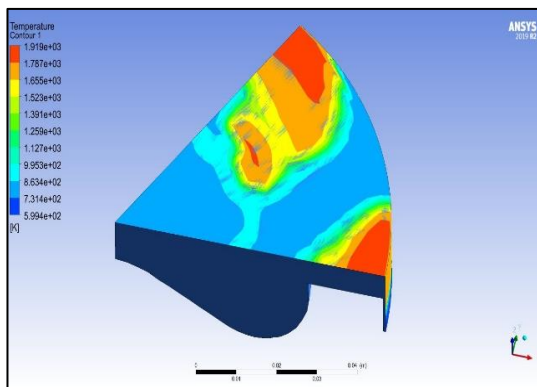


FIGURE 4.10(c): 75% biogas  
(1919K)

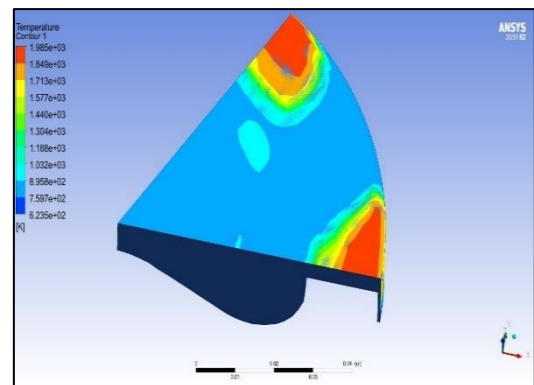


FIGURE 4.10(d): 70% biogas  
(1985K)

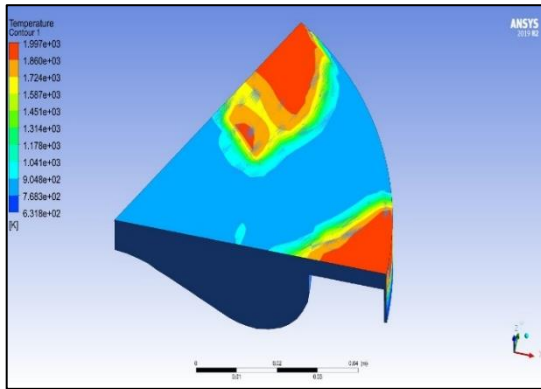


FIGURE 4.10(e): 65% biogas (1997K)

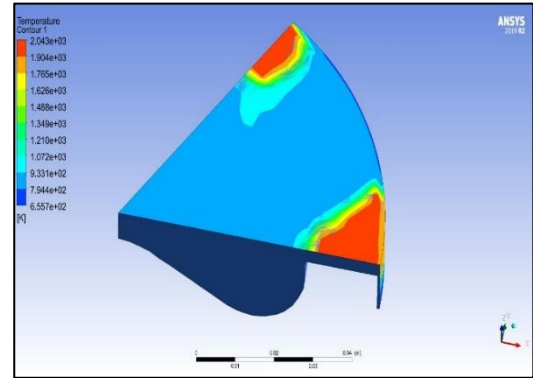


FIGURE 4.10(f): 60% biogas (2043K)

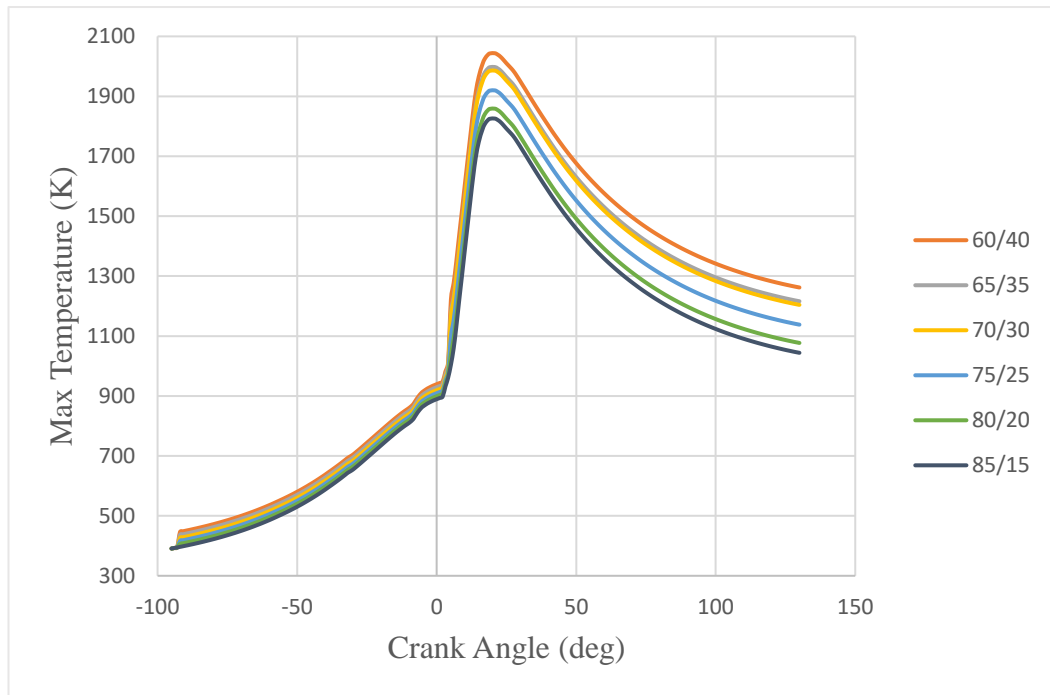


FIGURE 4.11: Maximum Temperature vs Crank Angle Diagram

Based on Figure 4.11, at 21 degrees crank angle from top dead centre, the 60/40 mix shows the highest maximum temperature obtained amongst all whereas the 85/15 mix is the lowest. However, the smallest deviation in maximum temperature is noticed between 65/35 and 70/30 mix. Between 70/30 and 75/25 mix, the largest gap in peak temperature is observed and found to be significant.

### 4.6.3 Effect of Biogas substitution on Rate of Heat Release (RoHR)

Based on contours from Figure 4.12(a) to 4.12(f), lower biogas substitution results in higher rate of heat energy released. This also means that turbulent kinetic energy drastically increases with lower percentage of diesel displacement by biogas due to higher injected pilot fuel (diesel) mass. As turbulence increases, more rapid and complete combustion is achieved together with enhanced flame front speeds, contributing to higher RoHR.

In dual fuel operation, the first stage is primarily the combustion of pilot fuel (diesel) and primary fuel (biogas) entrained in the diesel spray. The second stage, however, is where biogas combustion occurs by flame propagation from the ignition centres formed by the diesel spray. The second stage is where a significant amount of chemical heat release takes place due to biogas combustion. At intermediate loads, the chemical RoHR increases with decreasing biogas substitution. This explains the reason behind lower thermal efficiency in dual fuel operation at intermediate loads as compared to pure diesel mode.

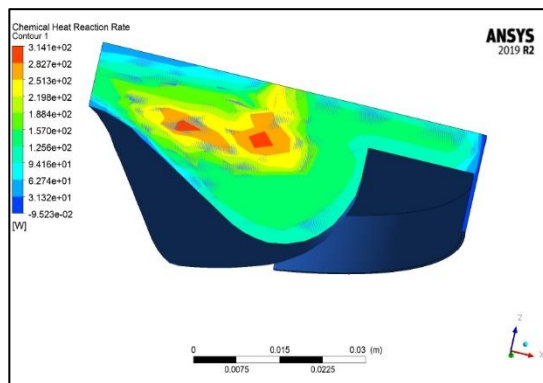


FIGURE 4.12(a): 85% biogas (314.1W)

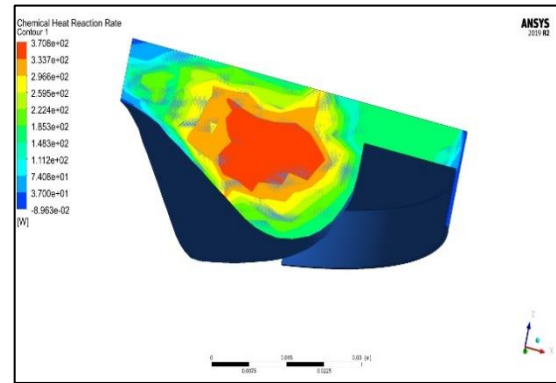


FIGURE 4.12(b): 80% biogas (370.8W)

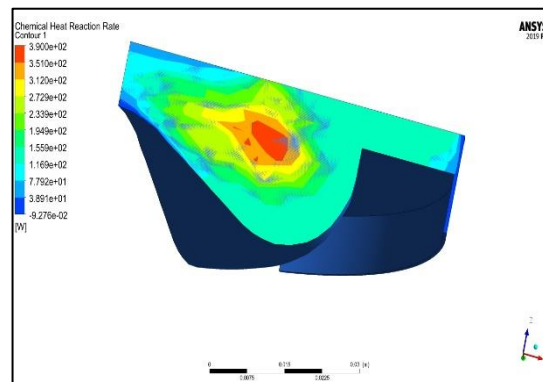


FIGURE 4.12(c): 75% biogas (390 W)

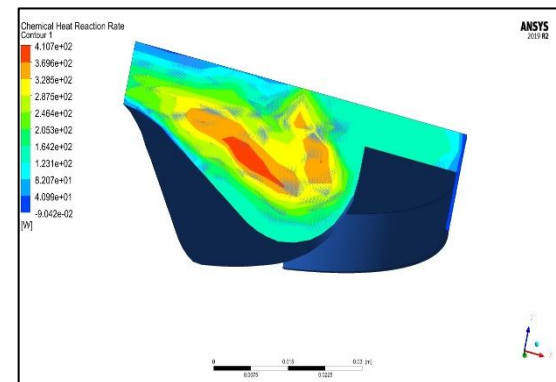


FIGURE 4.12(d): 70% biogas (410.7W)

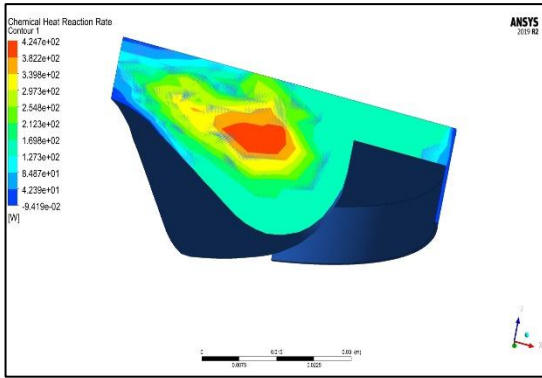


FIGURE 4.12(e): 65% biogas (424.7W)

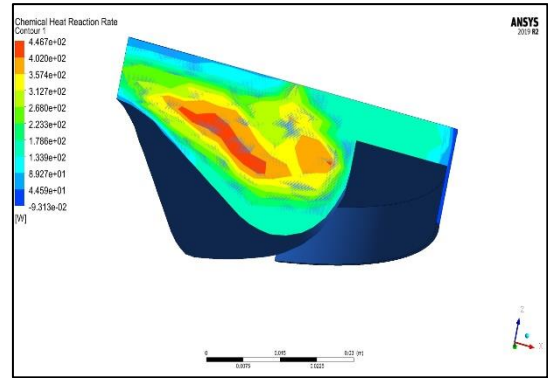


FIGURE 4.12(f): 60% biogas (446.7W)

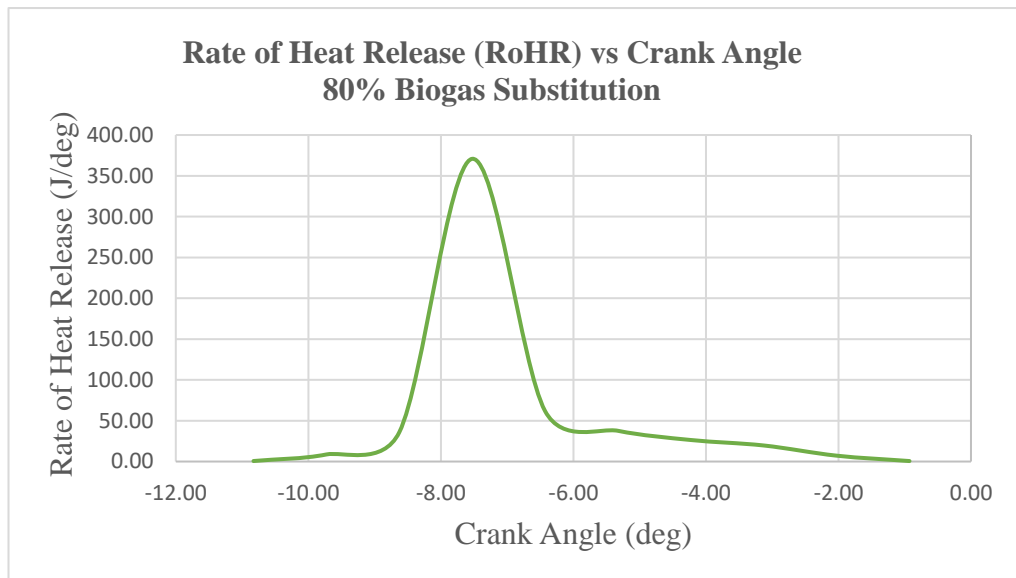


FIGURE 4.13: Rate of Heat Release (RoHR) vs Crank Angle at 80% biogas substitution

For validation of the chemical rate of heat release (RoHR), the results in Figure 4.13, at 80% biogas substitution was compared to the findings of Hussain [19] with the same compression ratio of 16:1. A similar trend was observed in the plot and the predicted results are well in conformity.

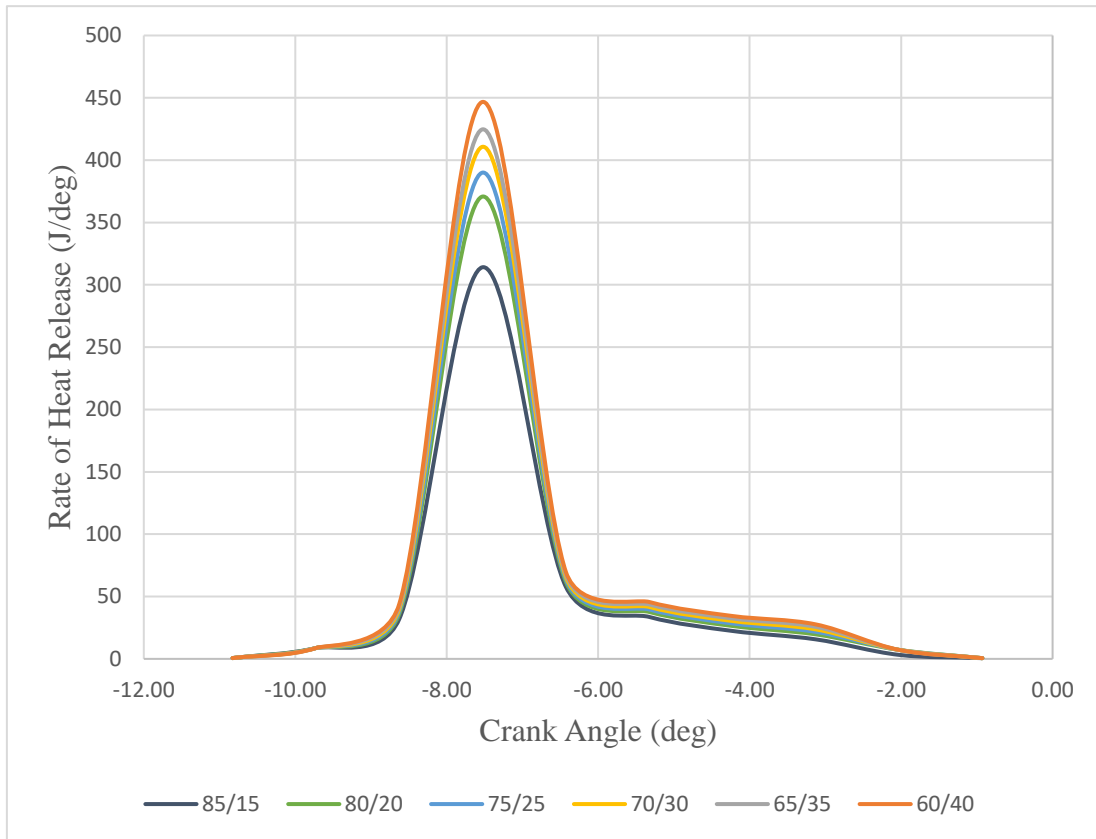


FIGURE 4.14: Rate of Heat Release (RoHR) vs Crank Angle for various Biogas-Diesel Compositions

Based on Figure 4.14, it can be observed that a higher RoHR is obtained from a lower biogas-diesel ratio at  $-14.6^{\circ}$ ATDC. The maximum deviation is large between 60/40 mix and 65/35 mix. From 65/35mix to 80/20 mix the maximum deviation is fairly constant. However, there is a very rapid declination observed from 80/20 mix to 85/15mix which prompt a further investigation to study the declination gradient in maximum RoHR.

A linear graph of maximum rate of heat release versus biogas-diesel ratio was plotted in Figure 4.15 and it was found that the slope between 80/20 mix and 85/15 mix was significantly steep. A conclusion was drawn that the RoHR will be largely compromised in the 85/15mix therefore the 80/20 mix is recommended as the maximum biogas substitution rate.

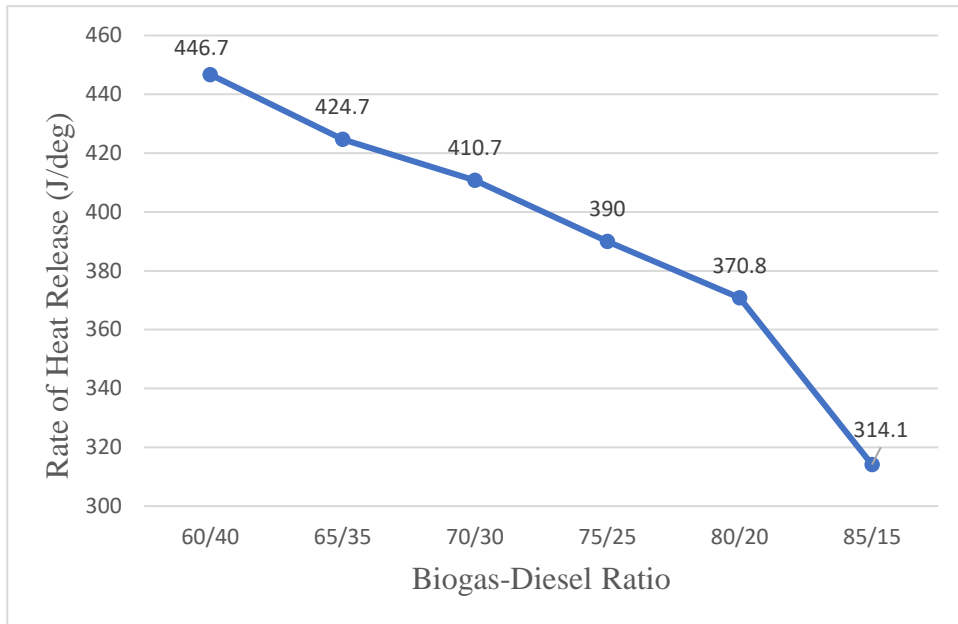


FIGURE 4.15: Maximum Rate of Heat Release (RoHR) vs various Biogas-Diesel Compositions

The heat release rate of 371 Joules at 80% biogas-20% diesel composition as shown in Figure 4.15 can be validated against the value obtained in the experimental setup of biogas-air premixture dual fuel engine used for comparison in the findings of Venu [18]. Hence, the results obtained from the CFD simulation is approximately similar to the experimental outcome. The 371 Joules heat release rate obtained is much lower than 580 Joules when compared to the experimental setup of natural gas-air premixture dual fuel engine [18]. Verification for this finding can be made based on the fact that the calorific value of biogas is about 24.5 MJ/kg, which is much lower when compared to that of natural gas which is about 48 MJ/kg. Similarly, the energy content [19] of biogas is 9.67 KWh for 1 Nm<sup>3</sup> when compared with natural gas of about 11 KWh for 1 Nm<sup>3</sup>.



#### 4.6.4 Comparison of Nitrogen Oxide (NO<sub>x</sub>) Emission between 80% Biogas-20% Diesel mix and Pure Diesel at 75% load

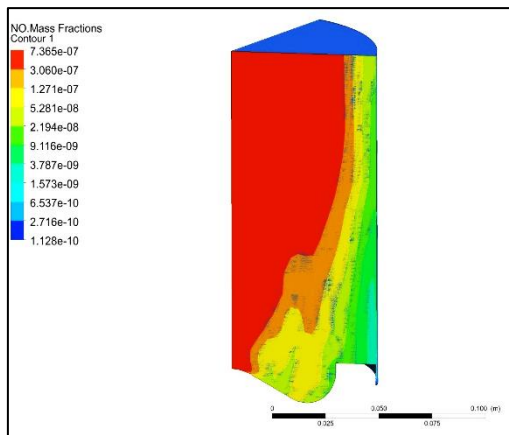


FIGURE 4.16(a): 100% pure diesel (7.365E-7 mass fraction)

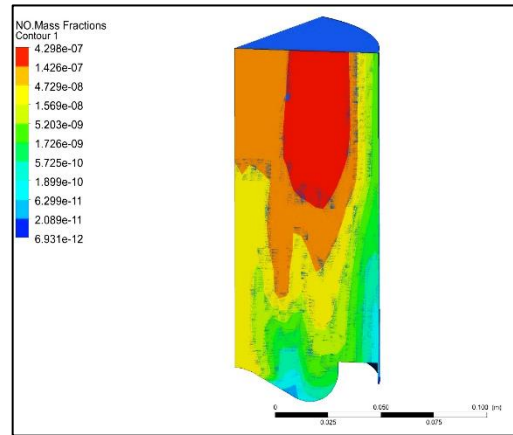


FIGURE 4.16(b): 80% biogas-20% diesel (4.298E-7 mass fraction)

Comparing Figure 4.16(a) with 4.16(b), approximately 42% NO<sub>x</sub> reduction (by mass) is achieved with 80/20 mix compared to pure diesel. NO<sub>x</sub> signifies a function of total oxygen within combustion chamber. The results of NO mass fractions can be validated against the research work of Yilmaz [22] and Mustafi [25] for conformance. The main reason for a significant NO<sub>x</sub> reduction in 80/20 dual fuel mix is because due to a high biogas substitution percentage in the mixture, the moisture (mass fraction of H<sub>2</sub>O) increases, which lowers the net combustion temperature. As the combustion temperature decreases, the NO<sub>x</sub> formation tendency reduces, which finally results in a significant reduction in NO<sub>x</sub> emissions for a 80% biogas-20% diesel composition. On the other hand, cases of pure diesel combustion resulted in significantly higher NO<sub>x</sub> emissions at 75% engine load compared to 80/20 dual fuel mix. This is because a full load diesel engine has faster injection timing and early ignition characteristics.

#### 4.6.5 Comparison of Carbon Monoxide (CO) Emission between 80% Biogas-20% Diesel mix and Pure Diesel at 75% load

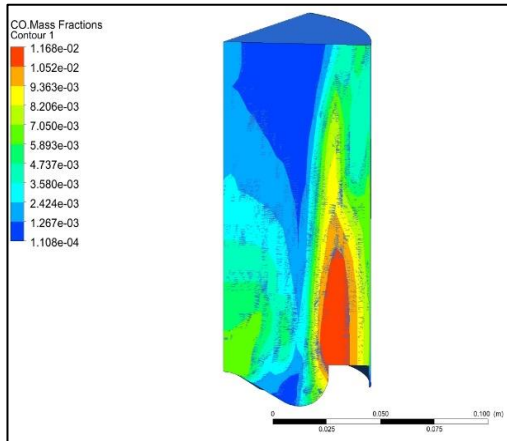


FIGURE 4.17(a): 100% pure diesel (1.168E-2 mass fraction)

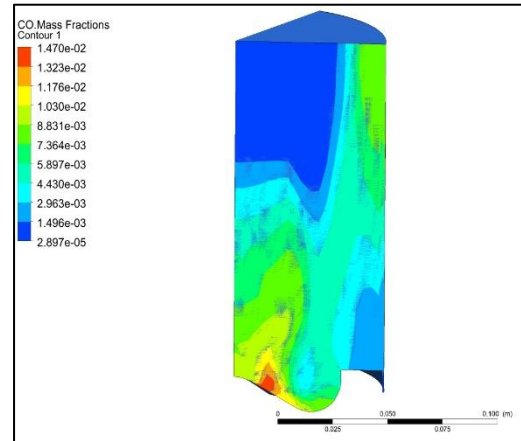


FIGURE 4.17(b): 80% biogas-20% diesel (1.47E-2 mass fraction)

By comparison between Figure 4.17(a) and 4.17(b), an approximate 26% CO increase (by mass) occurs with 80/20 mix compared to pure diesel. CO formation is an indicator of engine power loss. This is due to the fact that high percentage of biogas substitution requires lower cetane number which consequently decreases oxygen concentration in the combustion chamber thus producing lesser power in dual fuel operations. High methane mass fraction also contributes to high overall specific heat capacity and causes ignition delay to rise. Due to this reason, CO concentrations are higher in in dual-fuel compared to that of single- fuel combustion cases.

## 4.7 Economic Analysis

Economic analysis was carried out to determine the feasibility of the project proposal to be implemented in the future. This analysis also highlights how much reduction in operating costs is achievable if the wastefully open-flared biogas is resourcefully utilised as gaseous fuel for the diesel engine to drive the 648kW generator-set. Based on the simulation study performed, the maximum biogas substitution rate was found to be significantly high at 80% which concurrently indicates that a maximum of 80% diesel can be saved in operating the gen-set. In this analysis, calculation of operating costs was based solely on diesel fuel costs. For calculations purpose, the diesel price (as of January 2020) of RM 2.24/litre was used. Thereafter, calculations were made for the best dual-fuel composition which is 80% biogas-20% diesel as shown in Table 4.8.

TABLE 4.8: Yearly Diesel Fuel Consumption (648kW Gen Set)

Item	Data and Calculations	Description
1	Mill processing days = 26 days/month Maintenance day = 4 days/month (Sunday)	-
2	Gen-set operating hour = 1 hour/day (starting of process) Maintenance day = 12 hours/day (Sunday)	-
3	Diesel fuel consumption @ 75% load = 1.05 L/min @ RM 2.24/litre	Operating cost per hour = RM 141.12
4	Total gen-set operating hour = (26 days x 1 hour) + (4 days x 12 hours)	74 hrs/month
	<b>Average total diesel fuel consumption</b>	<b>RM 10,442.88 (per month)</b> <b>RM 125,314.56 (per year)</b>

<b>Diesel Savings (by dual fuel operation using 80% biogas-20% diesel)</b>	<b>= RM 10,442.88 x 80%</b>  <b>RM 8,354.30 (per month)</b>  <b>RM 100,251.65 (per year)</b>
--	--

Based on Table 4.8, it was found that operating the dual-fuel engine at intermediate load (75% engine load) using a 80/20 mix saves RM 8,354.30 of diesel on a monthly basis and RM 100,251.65 of diesel on a yearly basis. It is clear that operating the existing diesel generator-set on dual fuel mode provides substantial cost benefits through significant savings on diesel fuel cost.

## CHAPTER 5 : CONCLUSION AND RECOMMENDATION

### 5.1 Conclusion

This project was feasibly completed within the given period and a dissertation of this final year project topic was successfully produced with the noble guidance of my supervisor. The ultimate objective of this project was achieved which is to determine the maximum substitution level of diesel with biogas.

A CI engine with 648 kW power output was studied in pure diesel and dual-fuel mode with variants of six biogas-diesel compositions. In Part I of the results, theoretical calculations for brake thermal efficiency, specific fuel consumption and diesel displacement ratio were made to determine the most suitable engine load for dual fuel operation. The following conclusions were made for all cases. Brake thermal efficiency of the CI engine run in dual-fuel mode is lower than pure diesel mode. Specific fuel consumption in dual-fuel mode is higher than full load diesel operation and diesel displacement ratio increases with higher biogas substitution. Ultimately, the most suitable engine load was identified to be 75% (intermediate load).

Thereafter, in Part II, in-cylinder combustion simulation was carried out as per the existing gen-set engine specifications using ANSYS Forte. The main objective was to study engine performance characteristics using combustion parameters such as peak pressure, maximum temperature, chemical rate of heat release as well as emission characteristics such as NO<sub>x</sub> and CO formation. The results show:

1. In-cylinder peak pressure for dual fuel cases are in between 34-37 bars which is lower than that of pure diesel mode. As biogas substitution decreases, the peak pressure increases.
2. The maximum temperature for dual cases is in between 1825-2043K which show decrease as compared to full load diesel operation. As biogas substitution decreases, the maximum temperature increases.
3. Rate of heat release obtained for dual fuel cases is between 314-447 J/deg which is below that of pure diesel mode. This is the main reason for lower thermal efficiency in dual fuel cases as compared to pure diesel mode. At intermediate loads, the rate of heat release increases with lower biogas substitution. A substantially steep gradient was found between 80/20mix and 85/15mix. Hence,

the rate of heat release is be largely compromised in the 85/15mix therefore the 80% biogas is recommended as the maximum biogas substitution rate.

4. Emission characteristics analysis of dual fuel CI engine operation run in 80/20 mix proves that a significant 42% NO<sub>x</sub> reduction (by mass) can be achieved. However, it suffers from the problem of lower brake thermal efficiency and higher CO emissions at intermediate engine load due to poor ignition. As the reduction percentage in NO<sub>x</sub> outweighs the other emission parameters, it is proven that dual fuel gen-set operation is less polluting and more environmental friendly.

The combustion and exhaust emissions results conform well with experimental results and trends obtained from other researchers. Therefore, the CFD combustion simulation results are strongly validated. CFD simulation for dual fuel CI engines using ANSYS Forte is proven to be effective. Moreover, this simulation study is faster and much more cost effective in comparison to experimental setups and prototypes.

## **5.2 Recommendations**

Based on the critical findings from the simulation study and economic analysis, it is recommended that IOI Pukin Palm Oil Mill utilise the wastefully open-flared biogas for power generation on the existing generator set in dual fuel mode with a fuel composition of 80% Biogas-20% Diesel. To set up the 648kW diesel generator set in dual fuel mode, an external gas mixer is to be installed with a “T-junction” for entry of biogas inducted with air during the intake stroke into the combustion chamber. To improve brake thermal efficiency of the 80/20 mix, it is recommended to operate the dual fuel engine using a supercharged mixing system to boost thermal efficiency. The usage of more flexible pilot fuel mixtures with compressed biogas (CBG) is suggested to improve the performance and economic value of dual-fuel engines. Last but not least, investigation on the proposed dual fuel (80% biogas-20% diesel) engine stability and knocking is required as future work.

## REFERENCES

- [1] C. S. Khor and G. Lalchand, “A review on sustainable power generation in Malaysia to 2030: Historical perspective, current assessment, and future strategies,” *Renew. Sustain. Energy Rev.*, vol. 29, pp. 952–960, 2014.
- [2] C. P. Chien Bong *et al.*, “Review on the renewable energy and solid waste management policies towards biogas development in Malaysia,” *Renew. Sustain. Energy Rev.*, vol. 70, no. December 2016, pp. 988–998, 2017.
- [3] Energy Commission (Malaysia), “Energy Malaysia,” *Suruhanjaya Tenaga*, vol. 12, p. 3, 2017.
- [4] R. Ali, I. Daut, and S. Taib, “A review on existing and future energy sources for electrical power generation in Malaysia,” *Renew. Sustain. Energy Rev.*, vol. 16, no. 6, pp. 4047–4055, 2012.
- [5] M. Ohno, “Malaysian Palm Oil Council (Annual Report 2017),” *Phys. Rev.*, pp. 1–168, 2017.
- [6] J. C. Igwe and C. C. Onyegbado, “A Review of Palm Oil Mill Effluent ( Pome ) Water Treatment,” vol. 1, no. 2, pp. 54–62, 2007.
- [7] M. J. Chin, P. E. Poh, B. T. Tey, E. S. Chan, and K. L. Chin, “Biogas from palm oil mill effluent (POME): Opportunities and challenges from Malaysia’s perspective,” *Renew. Sustain. Energy Rev.*, vol. 26, pp. 717–726, 2013.
- [8] S. K. Loh, N. Abu Bakar, S. Mohamad Azri, B. Nurul Adela, T. Daryl Jay, and R. A. Stasha Eleanor, “Biogas Capture – A Means of Reducing Greenhouse Gas Emissions from Palm Oil Mill Effluent,” *Oil Palm Bull.*, vol. 75, no. November, pp. 27–36, 2017.
- [9] S. H. Shuit, K. T. Tan, K. T. Lee, and A. H. Kamaruddin, “Oil palm biomass as a sustainable energy source: A Malaysian case study,” *Energy*, vol. 34, no. 9, pp. 1225–1235, 2009.
- [10] S. M. Shafie, T. M. I. Mahlia, H. H. Masjuki, and A. Andriyana, “Current energy usage and sustainable energy in Malaysia: A review,” *Renew. Sustain. Energy Rev.*, vol. 15, no. 9, pp. 4370–4377, 2011.

- [11] A. C. Alkidas, "Heat transfer characteristics of a spark-ignition engine," *J. Heat Transfer*, vol. 102, no. 2, pp. 189–193, 1980.
- [12] S. H. Yoon and C. S. Lee, "Experimental investigation on the combustion and exhaust emission characteristics of biogas-biodiesel dual-fuel combustion in a CI engine," *Fuel Process. Technol.*, vol. 92, no. 5, pp. 992–1000, 2011.
- [13] J. O. Müller, D. S. Su, R. E. Jentoft, U. Wild, and R. Schlögl, "Diesel engine exhaust emission: Oxidative behavior and microstructure of black smoke soot particulate," *Environ. Sci. Technol.*, vol. 40, no. 4, pp. 1231–1236, 2006.
- [14] I. D. Bedoya, A. A. Arrieta, and F. J. Cadavid, "Effects of mixing system and pilot fuel quality on diesel-biogas dual fuel engine performance," *Bioresour. Technol.*, vol. 100, no. 24, pp. 6624–6629, 2009.
- [15] N. Gas, D. Engines, D. Fuel, and D. C. Jay, "Dual-Fuel Engine Latest Fuel Injection Systems on Medium Speed Engines used for IMO tier 3 requirements in devices for direct production of mechanical energy," no. 6, 2016.
- [16] N. Tippayawong, A. Promwungkwa, and P. Rerkkriangkrai, "Long-term operation of a small biogas/diesel dual-fuel engine for on-farm electricity generation," *Biosyst. Eng.*, vol. 98, no. 1, pp. 26–32, 2007.
- [17] N. H. S. Ray, "Biogas as Alternate Fuel in Diesel Engines: A Literature Review," *IOSR J. Mech. Civ. Eng.*, vol. 9, no. 1, pp. 23–28, 2013.
- [18] M. T. Thermal, "ISSN No : 2348-4845 CFD Simulation of Dual Fuel Natural Gas Based IC Engine Using Ansys ICE Package ISSN No : 2348-4845," vol. 3, no. July, pp. 501–506, 2016.
- [19] S. M. Hussain, A. Pradesh, and A. Pradesh, "CFD analysis of combustion and emissions to study the effect of compression ratio and biogas substitution in a diesel engine with experimental verification.," *Int. J. Eng. Sci. Technol.*, vol. 4, no. 2, pp. 473–492, 2012.
- [20] M. Dezfouli, "Diesel engine CFD simulations : investigation of time step on the combustion phenomena," pp. 1233–1237, 2018.
- [21] A. D. Canonsburg, "Forte Tutorials," no. August, 2017.



- [22] H. Koten, M. Yilmaz, and M. Zafer Gul, "Compressed biogas-diesel dual-fuel engine optimization study for ultralow emission," *Advances in Mechanical Engineering*, vol. 23, 2014.
- [23] N. N. Mustafi, R. R. Raine, and S. Verhelst, "Combustion and emissions characteristics of a dual fuel engine operated on alternative gaseous fuels," *Fuel*, vol. 109, pp. 669–678, 2013.
- [24] Caterpillar, "648 ekW 810 kVA 50 Hz 1500 rpm 400 Volts Caterpillar PRIME Diesel Generator Set , *European Sourced Catalogue* , pp. 2–6, November, 2016.
- [25] N. N. Mustafi and R. R. Raine, "A Study of the Emissions of a Dual Fuel Engine," vol.19, 2008.
- [26] Beale, J. C. and Reitz, R. D., "Modelling spray atomization with the Kelvin-Helmholtz/ Rayleigh-Taylor hybrid model," *Atomization and Sprays*, vol.9, pp. 623-650, 1999.
- [27] Wang, Y., Ge, H-W. and Reitz, R.D., "Validation of Mesh- and Timestep-Independent Spray Models for Multi-Dimensional Engine CFD Simulation," *SAE Int. J. Fuels Lubr*, vol.3, pp. 277-302, 2010.
- [28] Munnannur, A. and Reitz, R. D., "A Comprehensive Collision Model for Multi-Dimensional Engine Spray Computations," *Atomization and Sprays*, vol.19, pp 597-619, 2009.
- [29] Ra, Y. and Reitz, R. D., "A vaporization model for discrete multi-component fuel sprays," *International Journal of Multiphase Flow*, vol.35, pp.101-117, 2009.